

Effects of Wild-Type and Mutant Forms of Atrial Natriuretic Peptide on Atrial Electrophysiology and Arrhythmogenesis

Rui Hua, PhD*; Sarah L. MacLeod, MSc*; Iuliia Polina, PhD*; Motahareh Moghtadaei, PhD;
Hailey J. Jansen, MSc; Oleg Bogachev, MD; Stacy B. O'Blenes, MD; John L. Sapp, MD;
Jean-Francois Legare, MD; Robert A. Rose, PhD

Background—Atrial natriuretic peptide (ANP) is a hormone with numerous beneficial cardiovascular effects. Recently, a mutation in the ANP gene, which results in the generation of a mutant form of ANP (mANP), was identified and shown to cause atrial fibrillation in people. The mechanism(s) through which mANP causes atrial fibrillation is unknown. Our objective was to compare the effects of wild-type ANP and mANP on atrial electrophysiology in mice and humans.

Methods and Results—Action potentials (APs), L-type Ca^{2+} currents ($I_{\text{Ca,L}}$), and Na^+ current were recorded in atrial myocytes from wild-type or natriuretic peptide receptor C knockout (NPR- $\text{C}^{-/-}$) mice. In mice, ANP and mANP (10–100 nmol/L) had opposing effects on atrial myocyte AP morphology and $I_{\text{Ca,L}}$. ANP increased AP upstroke velocity (V_{max}), AP duration, and $I_{\text{Ca,L}}$ similarly in wild-type and NPR- $\text{C}^{-/-}$ myocytes. In contrast, mANP decreased V_{max} , AP duration, and $I_{\text{Ca,L}}$, and these effects were completely absent in NPR- $\text{C}^{-/-}$ myocytes. ANP and mANP also had opposing effects on $I_{\text{Ca,L}}$ in human atrial myocytes. In contrast, neither ANP nor mANP had any effect on Na^+ current in mouse atrial myocytes. Optical mapping studies in mice demonstrate that ANP sped electric conduction in the atria, whereas mANP did the opposite and slowed atrial conduction. Atrial pacing in the presence of mANP induced arrhythmias in 62.5% of hearts, whereas treatment with ANP completely prevented the occurrence of arrhythmias.

Conclusions—These findings provide mechanistic insight into how mANP causes atrial fibrillation and demonstrate that wild-type ANP is antiarrhythmic. (*Circ Arrhythm Electrophysiol.* 2015;8:1240-1254. DOI: 10.1161/CIRCEP.115.002896.)

Key Words: action potentials ■ atrial fibrillation ■ atrial natriuretic peptides ■ calcium channels ■ electrophysiology

Atrial fibrillation (AF) is a highly prevalent cardiac arrhythmia^{1,2} and is a major clinical problem because of the fact that current therapeutic approaches have significant limitations.³ AF, which is characterized by the rapid and irregular activation of the atria, can occur in association with many cardiovascular disorders (ie, heart failure and hypertension) or in the absence of structural disease (lone AF).^{4,5} Lone AF is known to occur in association with genetic mutations in, for example, ion channels and gap junction proteins.^{6–9}

Recently, a mutation in the *NPPA* gene, which encodes the cardioprotective hormone atrial natriuretic peptide (ANP),¹⁰ was identified and linked to the occurrence of AF.¹¹ This mutation is characterized by a 2-base pair deletion in exon 3, which causes a frameshift that abolishes the stop codon and extends the normal reading frame. This *NPPA* mutation results in the production of a 40-amino acid mutant ANP (mANP) consisting of the normal 28-amino acid ANP with an abnormal 12-amino acid carboxyl terminal extension.

ANP is one member of a family of NPs that also includes B-type NP (BNP) and C-type NP (CNP).^{10,12} ANP is produced

in atrial myocytes and is released into the circulation in response to atrial stretch. ANP is best known for its ability to regulate blood volume and blood pressure through effects in the kidneys (natriuresis and diuresis) and blood vessels (smooth muscle relaxation and endothelial permeability).¹⁰ We have recently demonstrated that NPs have potent effects on cardiac electrophysiology.^{13–16} For example, BNP and CNP can increase action potential (AP) duration (APD) in association with increases in L-type Ca^{2+} current ($I_{\text{Ca,L}}$) in atrial myocytes.¹³ We have also shown that wild-type NPs (BNP and CNP) can potentially increase electrical conduction in the sinoatrial node and atrial myocardium.¹⁷

Wild-type ANP is able to elicit its physiological effects by binding to 2 NP receptors (NPRs) called NPR-A and NPR-C.^{10,18,19} NPR-A is a particulate guanylyl cyclase receptor. When bound to ANP, NPR-A increases guanylyl cyclase activity and the production of cyclic GMP, which can modulate several downstream signaling proteins, including protein kinase G and phosphodiesterases.^{10,20} NPR-C is coupled to the activation of inhibitory G-proteins that reduce adenylyl

Received February 18, 2015; accepted July 10, 2015.

From the Department of Physiology and Biophysics (R.H., S.L.M., I.P., M.M., H.J.J., O.B., S.B.O., J.L.S., R.A.R.), IWK Health Centre (S.B.O.), Department of Surgery (S.B.O., J.-F.L.), Division of Cardiology (J.L.S.), School of Biomedical Engineering (R.A.R.), Faculty of Medicine, Dalhousie University, Halifax, Nova Scotia, Canada.

*Dr Hua, S.L. MacLeod, and Dr Polina contributed equally to this work.

The Data Supplement is available at <http://circep.ahajournals.org/lookup/suppl/doi:10.1161/CIRCEP.115.002896/-DC1>.

Correspondence Robert A. Rose, PhD, Department of Physiology and Biophysics, Dalhousie University, Sir Charles Tupper Medical Bldg – Room 4J, 5850 College St, PO Box 15000, Halifax, Nova Scotia, B3H 4R2, Canada. E-mail robert.rose@dal.ca

© 2015 American Heart Association, Inc.

Circ Arrhythm Electrophysiol is available at <http://circep.ahajournals.org>

DOI: 10.1161/CIRCEP.115.002896

WHAT IS KNOWN

- Atrial natriuretic peptide (ANP) is a powerful regulator of atrial function, including atrial electrophysiology.
- A mutation in the ANP gene results in the production of a mutant ANP that has been linked with atrial fibrillation in people; however, the mechanism(s) by which mutant ANP creates a substrate for atrial fibrillation are unknown.

WHAT THE STUDY ADDS

- Wild-type ANP and mutant ANP have opposing effects on atrial electrophysiology, including action potential morphology, L-type Ca^{2+} current, and atrial conduction velocity, via distinct receptor-mediated signaling mechanisms.
- Mutant ANP created a substrate for atrial arrhythmias that were associated with disorganized atrial activation patterns, multiple ectopic foci, and re-entrant conduction.
- Wild-type ANP was highly protective against atrial arrhythmias suggesting that ANP may be a target to prevent atrial fibrillation.

cyclase activity and intracellular cAMP (cAMP) levels.^{21,22} NPR-C activates inhibitory G-proteins through a specific inhibitory G-protein activator domain located in the 37-amino acid intracellular portion of the receptor.^{23,24}

mANP was found to circulate at concentrations 5 to 10× greater than wild-type ANP in patients affected by this mutation, and it has been hypothesized that this leads to enhanced effects of ANP that could create an electrophysiological substrate for AF.^{11,25} However, the ionic and molecular mechanism(s) through which mANP causes AF in humans are currently unknown. Accordingly, the goal of this study was to compare the effects of wild-type ANP and mANP on atrial electrophysiology in mouse and human atrial tissues. Our findings demonstrate that ANP and mANP have opposing effects on atrial electrophysiology because of the activation of distinct signaling pathways. These findings may explain how mANP leads to AF and also provide new insight into the electrophysiological effects of wild-type ANP in the atria.

Methods

An expanded Methods section is available in the Data Supplement.

Mice

This study used wild-type and NPR-C knockout (NPR-C^{-/-})^{14,26} mice between the ages of 10 to 15 weeks. All experimental procedures were approved by the Dalhousie University Committee for Laboratory Animals and followed the guidelines of the Canadian Council on Animal Care.

Human Tissue Samples and Patient Characteristics

Right atrial tissue samples were obtained from cardiac surgery patients who were in sinus rhythm and had no previous history of

arrhythmia. Patient characteristics are listed in Table I in the Data Supplement. All patients gave informed written consent to participate in our study, which was approved by the Research Ethics Board of the Capital Health District Authority.

Peptides

This study used wild-type ANP and mANP, which were both obtained from Bachem (Torrance, CA). mANP (amino acid sequence: SLRRSCFGGRMDRIGAQSGLCNSFRYRITAREDKQGWA)^{11,27} was synthesized and confirmed by mass spectrometry, amino acid analysis, and high-performance liquid chromatography by Bachem.

Patch Clamping of Atrial Myocytes From Mice and Humans

Right or left atrial myocytes were isolated from mice enzymatically as we have described previously.^{13,28} Human right atrial myocytes were isolated from tissue samples obtained from cardiac surgery patients using similar procedures to those in mice, with some specific modifications as outlined in the Data Supplement. Mouse and human atrial myocytes were used to record APs using the perforated patch-clamp technique and I_{CaL} and Na^+ current (I_{Na}) using the whole-cell patch-clamp technique. The solutions and experimental protocols for these experiments are available in the Data Supplement.

Quantitative Polymerase Chain Reaction

Quantitative gene expression in human right atrial samples was performed using approaches we have described previously.^{13,28} Intron spanning primers were designed for human NPR-A, NPR-B, NPR-C, and GAPDH. Experimental protocols and primer sequences are provided in the Data Supplement.

cAMP Assay

cAMP was measured in isolated mouse right atrial myocytes using an HTRF cAMP Femto2 kit (Cisbio) according to manufacturer's instruction (Data Supplement).

High-Resolution Optical Mapping

Patterns of electrical conduction, atrial effective refractory period (ERP), and susceptibility to arrhythmias were studied in isolated atrial preparations using optical mapping techniques we have previously described.^{17,28,29} Optical mapping was done using the voltage sensitive dye di-4-ANEPPS (10 μ mol/L) and blebbistatin (10 μ mol/L) to suppress contractile activity. All analyses were performed using custom software. Details are provided in the Data Supplement.

To measure ERP, atrial preparations were given an 8-stimulus drive train at a cycle length of 90 ms followed by a single extra stimulus at progressively shorter cycle lengths. ERP was defined as the shortest coupling interval allowing for capture of the atrial preparation.

For arrhythmia studies, we used S1–S2 pacing protocols in which the atria were paced at a fixed cycle length (90 ms) and then given 3 to 6 premature stimuli at progressively shorter cycle lengths (S2). The details for these experimental approaches are provided in the Data Supplement.

Statistical Analysis

All data are presented as mean \pm SD. Data were analyzed using a Student *t* test, 1-way ANOVA with Tukey post hoc test, 1-way repeated measures ANOVA with Tukey post hoc test, or Fisher exact test as indicated in each figure legend. $P < 0.05$ was considered significant.

Results

ANP and mANP Have Opposing Effects on Atrial Myocyte Electrophysiology in Mice

Although circulating concentrations of mANP were found to be higher than those of wild-type ANP in individuals who

have this *NPPA* mutation,¹¹ our goal was to determine whether ANP and mANP have distinct effects on atrial electrophysiology independent of differences in dose. Therefore, we initially measured the effects of identical doses of wild-type ANP (100 nmol/L) and mANP (100 nmol/L) on AP morphology in mouse right atrial myocytes in basal conditions (Figure 1A in the Data Supplement). These measurements demonstrate that neither ANP nor mANP had any effects on mouse atrial AP properties in basal conditions (Figure 1B and Tables II and III in the Data Supplement). Because we have previously shown that $I_{Ca,L}$ is a major target of NPs in the atria,^{13,15} we also measured the effects of ANP and mANP (100 nmol/L doses) on basal $I_{Ca,L}$ in mouse right atrial myocytes (Figure 1C and 1F in the Data Supplement). In agreement with the absence of effects on AP morphology, ANP and mANP had no effects on mouse atrial $I_{Ca,L}$ density (Figure 1D and 1G in the Data Supplement) or $I_{Ca,L}$ activation kinetics (Figure 1E and 1H; Tables IV and V in the Data Supplement) in basal conditions.

The absence of effects of ANP on AP morphology and $I_{Ca,L}$ in basal conditions is consistent with our previous studies showing that the related peptides BNP and CNP only affect mouse atrial myocyte electrophysiology in the presence of the β -adrenergic receptor agonist isoproterenol.¹³ Accordingly, we next measured the effects of ANP and mANP on AP morphology in mouse atrial myocytes after application of isoproterenol (10 nmol/L). In these experiments, ANP and mANP were each applied at doses of 10 and 100 nmol/L to consider the dose dependence of each of these peptides.

The effects of ANP (10 and 100 nmol/L) on mouse atrial AP morphology are illustrated in Figure 1. Representative recordings (Figure 1A and 1D) and summary data illustrate that isoproterenol increased ($P<0.05$) the AP maximum upstroke velocity (V_{max} ; Figure 1B and 1E) and APD at 50% (APD₅₀), 70% (APD₇₀), and 90% (APD₉₀) repolarization (Figure 1C and 1F). Application of ANP at both doses further increased ($P<0.05$) V_{max} (Figure 1B and 1E; Tables VI and VII in the Data Supplement) and APD at all repolarization times (Figure 1C and 1F; Tables VI and VII in the Data Supplement). There was no difference in the magnitude of the increases in V_{max} ($P=0.841$), APD₅₀ ($P=1.000$), APD₇₀ ($P=0.697$), or APD₉₀ ($P=0.146$) elicited by ANP at doses of 10 and 100 nmol/L (Figure 1G). The effects of ANP were fully reversible on washout.

Surprisingly, mANP (10 and 100 nmol/L) had the opposite effects to ANP on mouse atrial AP morphology. Representative recordings (Figure 2A and 2D) and summary data illustrate that after application of isoproterenol, mANP reversibly decreased ($P<0.05$) V_{max} (Figure 2B and 2E; Tables VIII and IX in the Data Supplement) and APD at all repolarization times (Figure 2C and 2F; Tables VIII and IX in the Data Supplement). There was no difference in the magnitude of the decreases in V_{max} ($P=0.112$), APD₅₀ ($P=0.289$), APD₇₀ ($P=0.525$), or APD₉₀ ($P=0.825$) elicited by mANP at doses of 10 and 100 nmol/L (Figure 2G).

The individuals affected by the *NPPA* mutation being studied were all heterozygous and thus produce both wild-type ANP and mANP.¹¹ Accordingly, we next studied the effects of ANP and mANP in combination on mouse atrial myocyte AP morphology. In these studies, we initially applied isoproterenol

(10 nmol/L) and then simultaneously applied ANP and mANP (100 nmol/L each). Representative AP recordings (Figure 3A) and summary data (Figure 3B and 3C) demonstrate that, in the presence of isoproterenol, combined application of equimolar doses of ANP and mANP had no effect on V_{max} ($P=0.070$), APD₅₀ ($P=0.387$), APD₇₀ ($P=0.127$), or APD₉₀ ($P=0.067$) although there was an overall trend toward a reduction in these AP parameters (Table X in the Data Supplement). These findings suggest that when present together at equal doses, the effects of ANP and mANP negate each other.

Next, we measured the effects of ANP and mANP (100 nmol/L each) on $I_{Ca,L}$ in the presence of isoproterenol (10 nmol/L) in mouse right atrial myocytes (Figure 4). Representative $I_{Ca,L}$ recordings (Figure 4A) and time course data (Figure 4B) demonstrate that isoproterenol increased atrial $I_{Ca,L}$ and subsequent application of ANP further augmented $I_{Ca,L}$. These effects were reversible on washout. The stimulatory effects of isoproterenol and ANP are also evident in summary current–voltage relationships (Figure 4C). The effects of ANP on atrial $I_{Ca,L}$ were further studied by performing steady-state conductance analysis (Figure 4D; Table XI in the Data Supplement). These measurements demonstrate that isoproterenol increased $I_{Ca,L}$ maximum conductance (G_{max}) in association with a negative shift ($P<0.05$) in the $V_{1/2}$ of channel activation ($V_{1/2(act)}$) from -10.2 ± 0.3 to -16.3 ± 1.1 mV. Application of ANP in the presence of isoproterenol further increased G_{max} ($P<0.05$) and shifted the $V_{1/2(act)}$ to -18.6 ± 1.1 mV ($P<0.05$).

Consistent with the AP data presented above, representative $I_{Ca,L}$ recordings (Figure 4E), time course data (Figure 4F), and summary current–voltage relationships (Figure 4G) demonstrate that mANP (100 nmol/L) had the opposite effects to ANP and decreased atrial $I_{Ca,L}$ in the presence of isoproterenol. Conductance analysis demonstrates that mANP decreased $I_{Ca,L}$ and G_{max} ($P<0.05$) and shifted the $V_{1/2(act)}$ ($P<0.05$) to more positive membrane potentials (Figure 4H; Table XII in the Data Supplement). Thus, as was the case for AP measurements, ANP and mANP have distinct and opposing effects on atrial $I_{Ca,L}$.

To assess the dose dependence of the effects of ANP and mANP on atrial $I_{Ca,L}$, we measured the effects of each peptide at concentrations between 1 and 100 nmol/L (in the presence of isoproterenol) on peak right atrial $I_{Ca,L}$ (Figure 2 in the Data Supplement). These studies demonstrate that ANP and mANP modulated $I_{Ca,L}$ at each dose tested. There was no significant difference in the magnitude of the effects of ANP ($P=0.30$) and mANP ($P=0.10$) at doses of 10 and 100 nmol/L although there was a trend toward larger effects at the higher dose. In contrast, the effects of ANP and mANP at 1 nmol/L doses were smaller ($P<0.05$) than those of ANP and mANP at the higher 2 doses. We also measured the effects of ANP and mANP (100 nmol/L each) on $I_{Ca,L}$ in mouse left atrial myocytes (Figure 3 in the Data Supplement). These data illustrate that the effects of ANP and mANP on $I_{Ca,L}$ are similar in right and left atrial myocytes.

Because ANP and mANP had opposing effects on AP V_{max} , which is importantly influenced by I_{Na} , we also measured the effects of isoproterenol (10 nmol/L) and each peptide (100 nmol/L) on mouse atrial I_{Na} (Figure 4 and Table XIII and

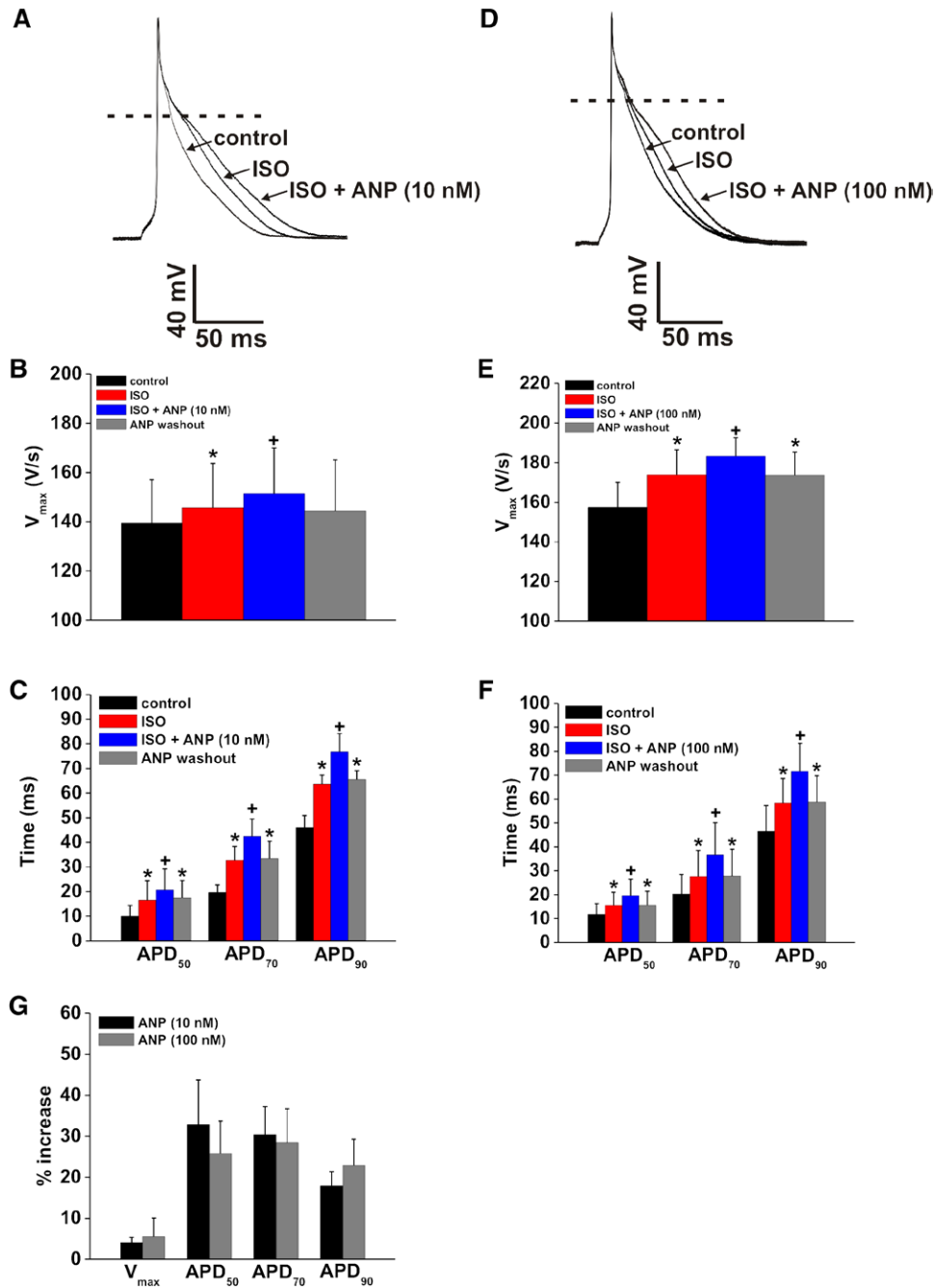


Figure 1. Effects of atrial natriuretic peptide (ANP) on mouse atrial action potential morphology in the presence of isoproterenol (ISO). ISO was applied at a dose of 10 nmol/L, and 2 doses of ANP (10 and 100 nmol/L) were studied. **A** and **D**, Representative right atrial action potentials (APs) in control conditions, in the presence of ISO (10 nmol/L), and after application of ANP (10 or 100 nmol/L) in the presence of ISO. Dashed lines are at 0 mV. **B** and **E**, Summary of the effects of ISO and ANP on right atrial AP upstroke velocity (V_{max}). **C** and **F**, Summary of the effects of ISO and ANP on right atrial AP duration (APD) at 50% (APD₅₀), 70% (APD₇₀), and 90% (APD₉₀) repolarization. * $P < 0.05$ vs control and + $P < 0.05$ vs ISO by 1-way repeated measures ANOVA with Tukey post hoc test; $n = 5$ myocytes for the 10 nmol/L dose of ANP; $n = 6$ myocytes for the 100 nmol/L dose of ANP. **G**, Summary of the percent increase in right atrial AP parameters elicited by 10 nmol/L and 100 nmol/L doses of ANP (in the presence of ISO). There was no significant difference in the magnitude of the effects of ANP at these 2 doses (data analyzed by Student t test). In this and all subsequent figures, summary data are presented as mean \pm SD. Analysis of additional AP parameters is provided in Tables VI and VII in the Data Supplement.

XIV in the Data Supplement). I_{Na} current-voltage relationships and steady-state conductance analysis demonstrate that neither isoproterenol, ANP, or mANP had any effects on atrial I_{Na} , suggesting that $I_{Ca,L}$ is the key ion channel regulated by these peptides (Discussion).

Role of NPR-A and NPR-C in Mediating the Effects of ANP and mANP on $I_{Ca,L}$

We have previously demonstrated that NPs (BNP and CNP) can modulate $I_{Ca,L}$ via the guanylyl cyclase-linked NPR-A/B receptors and NPR-C.^{13,22} Furthermore, ANP and mANP have

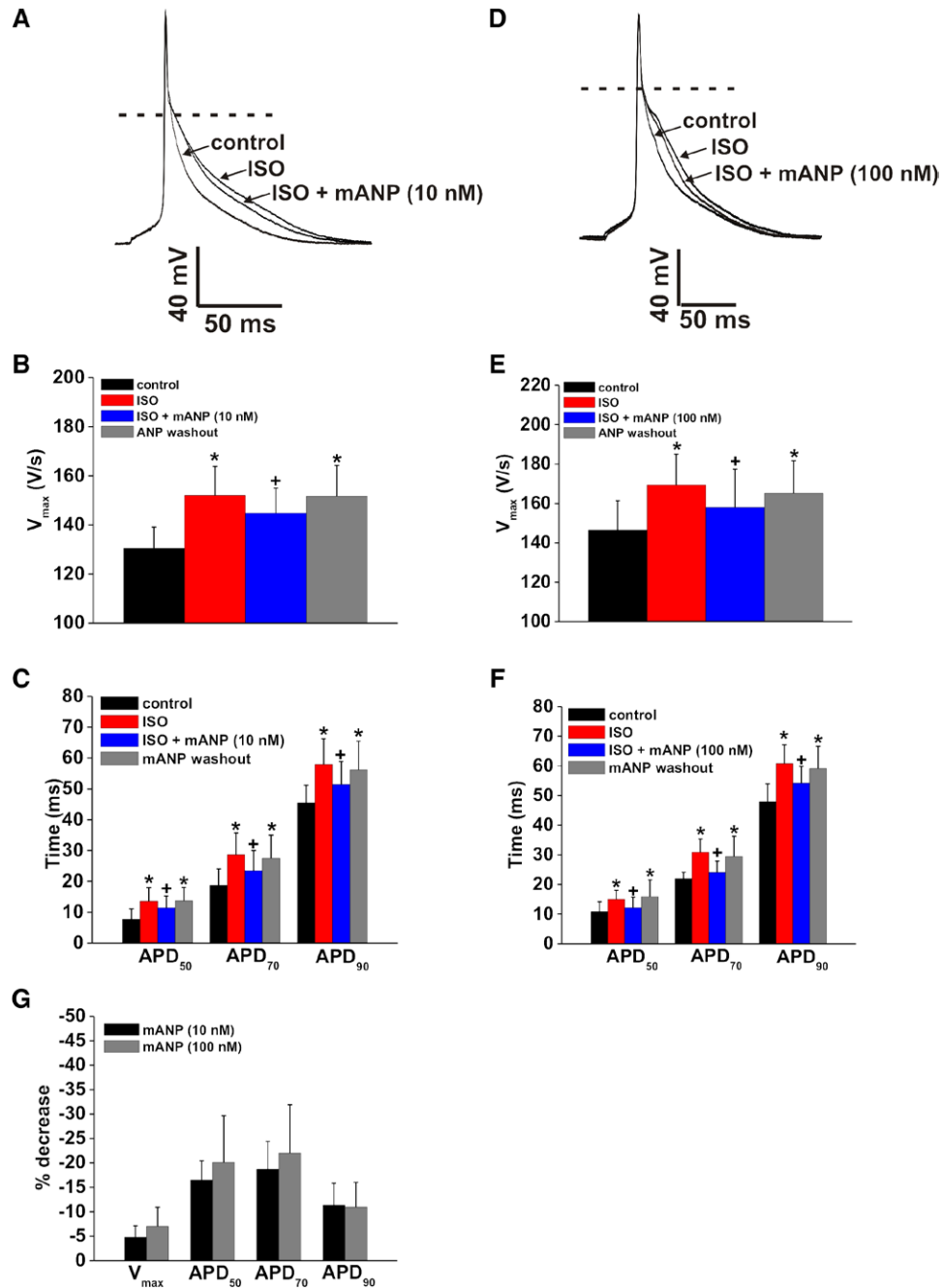


Figure 2. Effects of mutant atrial natriuretic peptide (mANP) on mouse atrial action potential (AP) morphology in the presence of isoproterenol (ISO). ISO was applied at a dose of 10 nmol/L, and 2 doses of mANP (10 and 100 nmol/L) were studied. **A** and **D**, Representative right atrial APs in control conditions, in the presence of ISO (10 nmol/L), and after application of mANP (10 or 100 nmol/L) in the presence of ISO. Dashed lines are at 0 mV. **B** and **E**, Summary of the effects of ISO and mANP on right atrial V_{max} . **C** and **F**, Summary of the effects of ISO and mANP on right atrial AP duration (APD) at APD₅₀, APD₇₀, and APD₉₀. * $P < 0.05$ vs control and † $P < 0.05$ vs ISO by 1-way repeated measures ANOVA with Tukey post hoc test; $n = 7$ myocytes for the 10 nmol/L dose of mANP; $n = 9$ myocytes for the 100 nmol/L dose of mANP. **G**, Summary of the percent decrease in right atrial AP parameters elicited by 10 nmol/L and 100 nmol/L doses of mANP (in the presence of ISO). There was no significant difference in the magnitude of the effects of mANP at these 2 doses (data analyzed by Student t test). Analysis of additional AP parameters is provided in Tables VIII and IX in the Data Supplement.

each been shown to bind NPR-A and NPR-C.²⁷ To determine the mechanism for the opposing effects of ANP and mANP on atrial $I_{Ca,L}$, we measured the effects of these 2 peptides (100 nmol/L doses) on $I_{Ca,L}$ (in the presence of isoproterenol; 10 nmol/L) in right atrial myocytes from NPR-C^{-/-} mice (Figure 5). These data demonstrate that ANP (Figure 5A–5C) increased isoproterenol-stimulated $I_{Ca,L}$ and that the magnitude

of the effect of ANP was similar to that observed in wild-type mice (compare with Figure 4).

Strikingly, the inhibitory effects of mANP on $I_{Ca,L}$ (in the presence of isoproterenol) were completely absent in atrial myocytes from NPR-C^{-/-} mice. The data in Figure 5D–5F demonstrate that isoproterenol increased $I_{Ca,L}$ as expected but mANP had no effects on $I_{Ca,L}$ density. Thus, the ability of ANP

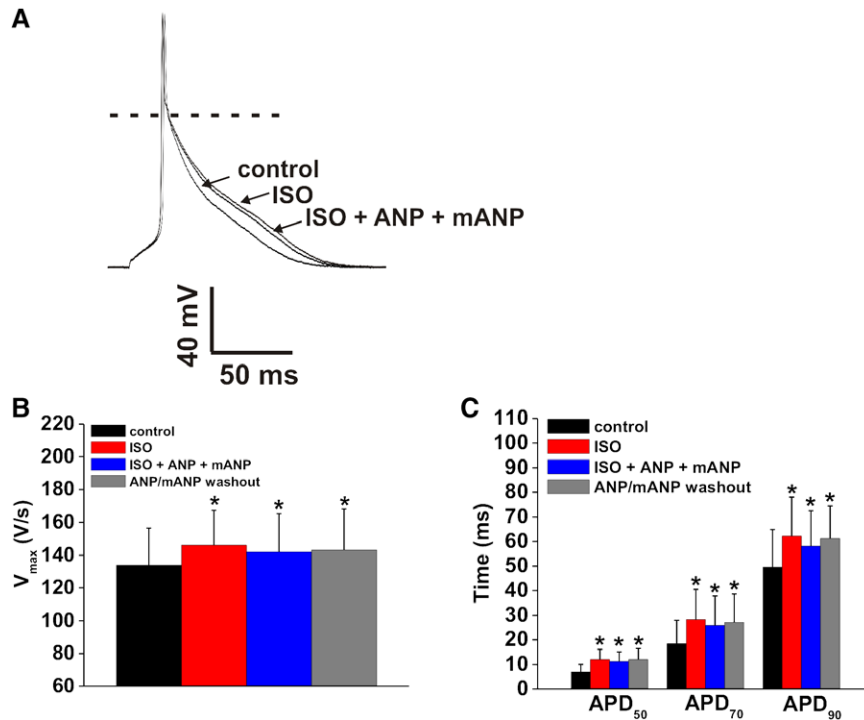


Figure 3. Effects of combined application of atrial natriuretic peptide (ANP) and mutant ANP (mANP) on mouse atrial action potential (AP) morphology in the presence of isoproterenol (ISO). **A**, Representative right atrial APs in control conditions, in the presence of ISO (10 nmol/L), and after application of ANP and mANP together (100 nmol/L each) in the presence of ISO. Dashed lines are at 0 mV. **B**, Summary of the effects of ISO and ANP+mANP on right atrial V_{max}. **C**, Summary of the effects of ISO and ANP+mANP on right atrial AP duration (APD) at APD₅₀, APD₇₀, and APD₉₀. *P<0.05 vs control; combined application of ANP and mANP had no significant effect on AP parameters; data were analyzed by 1-way repeated measures ANOVA with Tukey post hoc test; n=7 myocytes. Analysis of additional AP parameters is provided in Table X in the Data Supplement.

to increase I_{Ca,L} is maintained in NPR-C^{-/-} atrial myocytes, whereas the inhibitory effect of mANP on I_{Ca,L} is absent in mice lacking NPR-C receptors. This suggests that ANP and mANP signal via separate pathways.

Because the stimulatory effect of ANP on atrial I_{Ca,L} was maintained in NPR-C^{-/-} atrial myocytes, we hypothesized that this effect must be mediated by NPR-A, the only other receptor that ANP binds to physiologically.¹⁰ This hypothesis was tested using the NPR-A antagonist A71915.³⁰ We have previously demonstrated that A71915 has no direct effects on atrial I_{Ca,L}¹³; therefore, we applied A71915 (500 nmol/L) concomitantly with isoproterenol (10 nmol/L) for 5 minutes followed by application of ANP (100 nmol/L) in mouse right atrial myocytes. These data (Figure V in the Data Supplement) demonstrate that A71915 completely blocked the ability of ANP to increase atrial I_{Ca,L}.

ANP and mANP Have Opposing Effects on cAMP Production in Mouse Atrial Myocytes

The data described above demonstrate that ANP increases I_{Ca,L} via NPR-A, whereas mANP decreases I_{Ca,L} via NPR-C. We have previously demonstrated that NPR-A-mediated increases in I_{Ca,L} involve the inhibition of phosphodiesterase-3 (PDE3) by cyclic GMP,¹³ which would increase cAMP by preventing its hydrolysis. Conversely, NPR-C activation is known to reduce cAMP levels via the activation of inhibitory G-proteins.^{23,31} Accordingly, we hypothesized that the effects of ANP would be associated with increased cAMP

levels, whereas the effects of mANP would be associated with decreased cAMP production. This was tested using a cAMP assay in isolated mouse right atrial myocytes. In these experiments (Figure VI in the Data Supplement), the effects of ANP (100 nmol/L) and mANP (100 nmol/L) on intracellular cAMP levels were measured in basal conditions and in the presence of isoproterenol (10 nmol/L).

Consistent with an absence of effects on mouse atrial myocyte electrophysiology (AP morphology, I_{Ca,L}) in basal conditions, neither ANP (P=0.463) nor mANP (P=0.445) had any effect on cAMP concentrations in the absence of isoproterenol. In contrast, in the presence of isoproterenol, ANP and mANP had opposing effects on intracellular cAMP concentrations. Specifically, isoproterenol increased (P<0.05) cAMP as expected. Application of ANP in the presence of isoproterenol resulted in a further increase in cAMP (P<0.05), whereas application of mANP in the presence of isoproterenol resulted in lower cAMP concentrations (P<0.05). Thus, the opposing effects of ANP and mANP on atrial myocyte electrophysiology (in the presence of isoproterenol) occur in association with opposing effects of these 2 peptides on intracellular cAMP concentrations.

Effects of ANP and mANP on Human Right Atrial Myocyte I_{Ca,L}

The next set of experiments sought to translate our findings in mouse atrial myocytes to the human heart. Using quantitative polymerase chain reaction, we assessed the mRNA expression

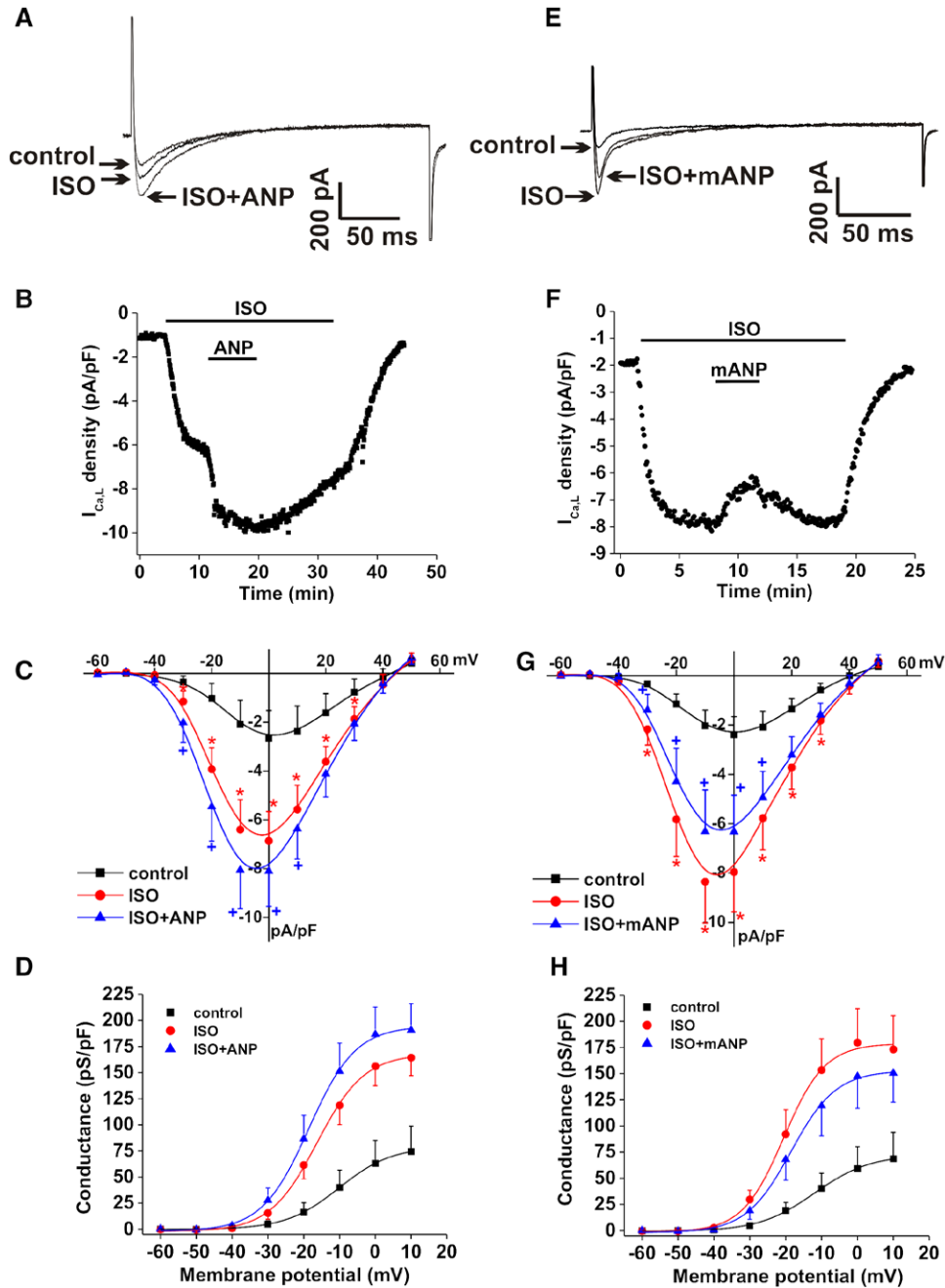


Figure 4. Effects of atrial natriuretic peptide (ANP) and mutant ANP (mANP) on mouse right atrial L-type Ca²⁺ currents (*I*_{Ca,L}) in the presence of isoproterenol (ISO). **A**, Representative right atrial *I*_{Ca,L} recordings in control conditions, in the presence of ISO (10 nmol/L), and after application of ANP (100 nmol/L) in the presence of ISO. **B**, Time course of the effects of ISO and ANP on *I*_{Ca,L}. **C**, Right atrial *I*_{Ca,L} *I*-*V* relationships in control conditions, in the presence of ISO, and after application of ANP in the presence of ISO. **P*<0.05 vs control and +*P*<0.05 vs ISO by 1-way repeated measures ANOVA with Tukey post hoc test; n=8 myocytes. **D**, Summary *I*_{Ca,L} conductance density plots demonstrating the effects of ISO and ANP on *I*_{Ca,L} activation kinetics. Analysis of *I*_{Ca,L} activation kinetics is provided in Table XI in the Data Supplement. **E**, Representative right atrial *I*_{Ca,L} recordings in control conditions, in the presence of ISO (10 nmol/L), and after application of mANP (100 nmol/L) in the presence of ISO. **F**, Time course of the effects of ISO and mANP on *I*_{Ca,L}. **G**, Right atrial *I*_{Ca,L} *I*-*V* relationships in control conditions, in the presence of ISO, and after application of mANP in the presence of ISO. **P*<0.05 vs control and +*P*<0.05 vs ISO by 1-way repeated measures ANOVA with Tukey post hoc test; n=6 myocytes. **H**, Summary *I*_{Ca,L} conductance density plots demonstrating the effects of ISO and mANP on *I*_{Ca,L} activation kinetics. Analysis of *I*_{Ca,L} activation kinetics is provided in Table XII in the Data Supplement.

pattern of all 3 NPRs in human right atrial samples obtained from patients undergoing cardiac surgery (Figure VII in the Data Supplement). These measurements demonstrate that all 3 NPRs are expressed in human right atrium and that NPR-C is more highly expressed (*P*<0.05) than NPR-A and NPR-B.

We also isolated atrial myocytes from human right atrial appendage samples and measured the effects of identical doses of ANP (100 nmol/L) and mANP (100 nmol/L) on human right atrial *I*_{Ca,L} in baseline conditions and in the presence of isoproterenol (10 nmol/L). Human *I*_{Ca,L} was recorded

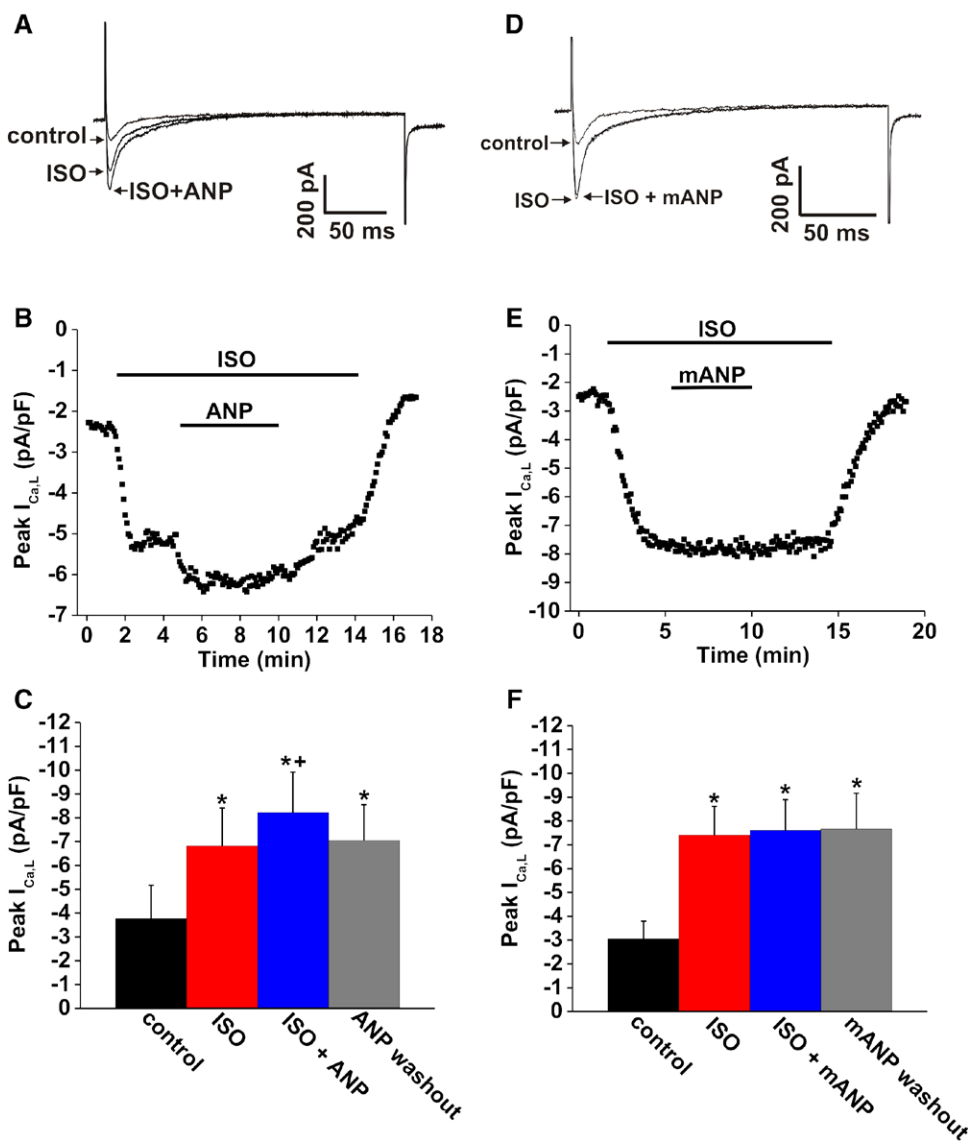


Figure 5. Effects of mutant atrial natriuretic peptide (mANP) on atrial L-type Ca^{2+} currents ($I_{Ca,L}$) are absent in myocytes from natriuretic peptide receptor C knockout (NPR-C^{-/-}) mice. **A**, Representative $I_{Ca,L}$ recordings (measured at 0 mV) illustrating the effects of isoproterenol (ISO; 10 nmol/L) and ANP (100 nmol/L) on right atrial myocytes from NPR-C^{-/-} mice. **B**, Time course of the effects of ISO and ANP on $I_{Ca,L}$ in NPR-C^{-/-} myocytes. **C**, Summary of the effects of ISO and ANP on peak $I_{Ca,L}$ in NPR-C^{-/-} right atrial myocytes. * P <0.05 vs control and + P <0.05 vs ISO by 1-way repeated measures ANOVA with Tukey post hoc test; n =6 myocytes. **D**, Representative $I_{Ca,L}$ recordings (at 0 mV) illustrating the effects of ISO (10 nmol/L) and mANP (100 nmol/L) in right atrial myocytes from NPR-C^{-/-} mice. **E**, Time course of the effects of ISO and mANP on $I_{Ca,L}$ in NPR-C^{-/-} myocytes. **F**, Summary of the effects of ISO and mANP on peak $I_{Ca,L}$ in NPR-C^{-/-} right atrial myocytes. * P <0.05 vs control by 1-way repeated measures ANOVA with Tukey post hoc test; mANP had no effect on $I_{Ca,L}$ amplitude in NPR-C^{-/-} atrial myocytes (P =0.989); n =9 myocytes.

using the same voltage clamp protocols used in our mouse recordings. Figure VIII in the Data Supplement illustrates a representative example of a family of $I_{Ca,L}$ recordings at membrane potentials between -60 and +60 mV along with the human $I_{Ca,L}$ current-voltage relationship, which was similar to that measured in mouse atrial myocytes (Figure I in the Data Supplement; Figure 4).

Representative $I_{Ca,L}$ recordings (Figure 6A) and summary data (Figure 6B) illustrate that ANP reversibly increased basal $I_{Ca,L}$ in human atrial myocytes. The magnitude of this effect was comparable with that seen in mice. Notably, however, this stimulatory effect of ANP on human atrial $I_{Ca,L}$ was observed without the requirement for prestimulation with isoproterenol. Next,

we measured the effects of mANP on basal $I_{Ca,L}$ in human right atrial myocytes. Representative recordings (Figure 6C) and summary data (Figure 6D) demonstrate that, as in the mouse, mANP had no effect on $I_{Ca,L}$ density in human atrial myocytes in the absence of isoproterenol. Finally, we measured the effects of ANP and mANP on human right atrial $I_{Ca,L}$ in the presence of isoproterenol (10 nmol/L; Figure 6E-6H). Consistent with our findings in mouse myocytes, ANP increased (P <0.05) isoproterenol-stimulated $I_{Ca,L}$, whereas mANP inhibited (P <0.05) isoproterenol-stimulated $I_{Ca,L}$ in human atrial myocytes. These effects of ANP and mANP were fully reversible after washout.

Our findings in human right atrial myocytes demonstrate that, similar to the mouse, the main effect of ANP is

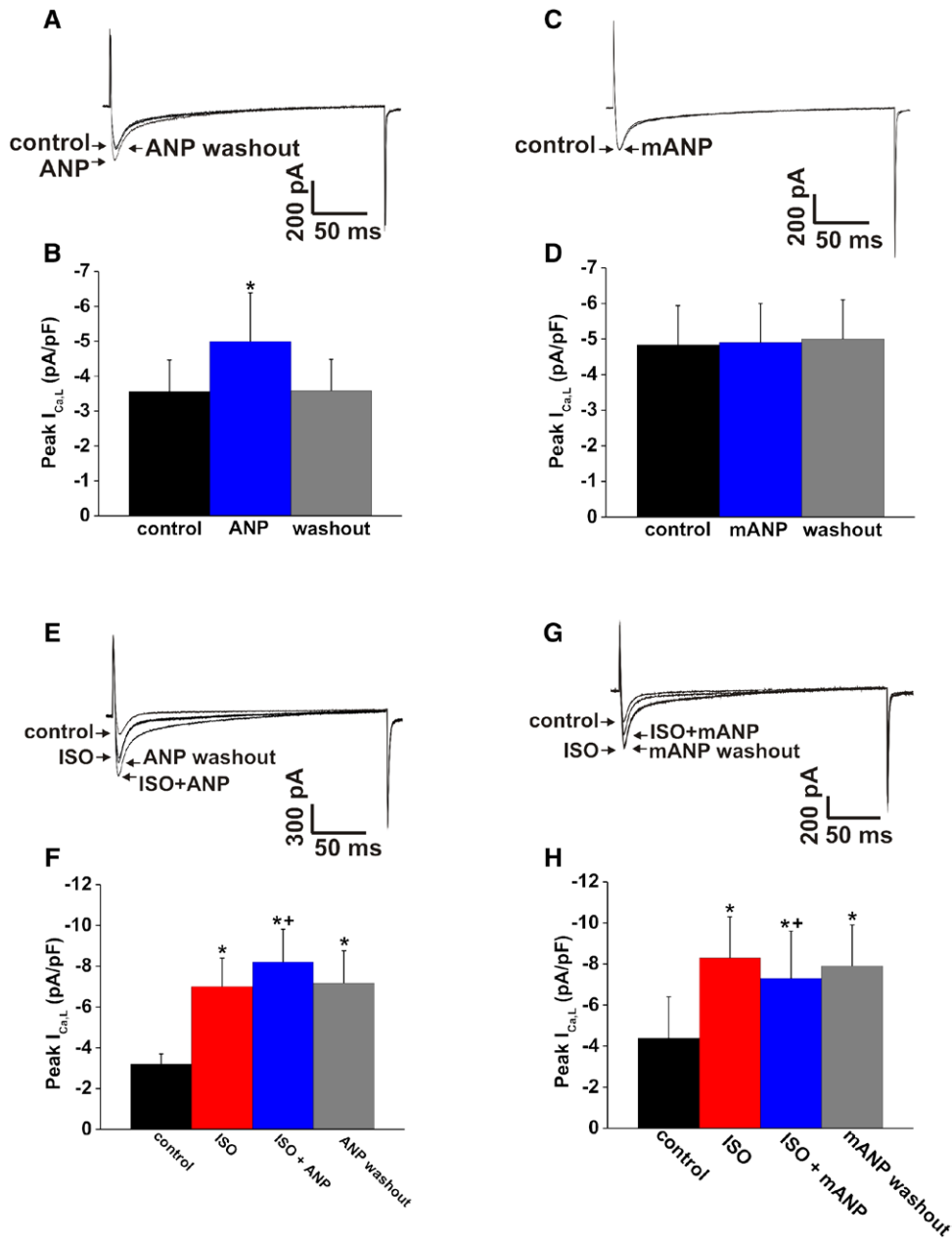


Figure 6. Effects of atrial natriuretic peptide (ANP) and mutant ANP (mANP) on L-type Ca^{2+} currents ($I_{Ca,L}$) in human right atrial myocytes in baseline conditions and in the presence of isoproterenol (ISO). **A**, Representative $I_{Ca,L}$ recordings (measured at 0 mV) in control conditions, after application of ANP (100 nmol/L), and after ANP washout. **B**, Summary data illustrating the effects of ANP on human atrial $I_{Ca,L}$ in basal conditions. * $P < 0.05$ vs control by 1-way repeated measures ANOVA with Tukey post hoc test; $n = 6$ myocytes from 3 patient samples. **C**, Representative $I_{Ca,L}$ recordings in control conditions and after application of mANP (100 nmol/L). **D**, Summary data illustrating that mANP had no effect ($P = 0.936$) on human atrial $I_{Ca,L}$ in basal conditions. Data were analyzed by 1-way repeated measures ANOVA; $n = 8$ myocytes from 4 patient samples. **E**, Representative $I_{Ca,L}$ recordings in control conditions, in the presence of ISO (10 nmol/L), after application of ANP (100 nmol/L) in the presence of ISO, and after ANP washout. **F**, Summary data illustrating the effects of ANP on human atrial $I_{Ca,L}$ in the presence of ISO. * $P < 0.05$ vs control and + $P < 0.05$ vs ISO by 1-way repeated measures ANOVA with Tukey post hoc test; $n = 6$ myocytes from 4 patient samples. **G**, Representative $I_{Ca,L}$ recordings in control conditions, in the presence of ISO (10 nmol/L), after application of mANP (100 nmol/L) in the presence of ISO, and after mANP washout. **H**, Summary data illustrating the effects of mANP on human atrial $I_{Ca,L}$ in the presence of ISO. * $P < 0.05$ vs control and + $P < 0.05$ vs ISO by 1-way repeated measures ANOVA with Tukey post hoc test; $n = 7$ myocytes from 4 patient samples.

to increase $I_{Ca,L}$, whereas mANP decreases $I_{Ca,L}$; however, a notable difference was that ANP was able to stimulate $I_{Ca,L}$ in basal conditions and in the presence of isoproterenol in human atrial myocytes, whereas in mice, ANP only increased $I_{Ca,L}$ in the presence of isoproterenol. We have previously shown that BNP and CNP (NPs closely related to ANP) also increase

mouse atrial $I_{Ca,L}$ in the presence of isoproterenol but not in basal conditions and that this is because mouse atria do not have constitutive PDE3 activity, which is necessary for the stimulatory effects of these NPs on atrial $I_{Ca,L}$.^{13,32}

On the basis of this, we hypothesized that human atrial myocytes must have constitutive PDE3 activity, which would

explain the ability of ANP to increase human atrial I_{CaL} in basal conditions. To test this hypothesis, we measured the effects of the PDE3 inhibitor milrinone (10 μ mol/L) on basal I_{CaL} in human right atrial myocytes (Figure IX in the Data Supplement). These data illustrate that milrinone potently, and reversibly, increased human atrial I_{CaL} confirming that, unlike the mouse,³² human atrial myocytes display constitutive PDE3 activity.

ANP and mANP Have Opposing Effects on Electrical Conduction in the Mouse Atria

Alterations in electrical conduction within the atria can contribute importantly to susceptibility to AF^{4,33}; therefore, we used high-resolution optical mapping to determine the effects of ANP and mANP on activation patterns in the mouse atria. These studies were performed in an isolated atrial preparation^{17,34,35} (Figure X in the Data Supplement) and used an intermediate dose of ANP (50 nmol/L) and mANP (50 nmol/L). Representative activation maps are presented in control conditions, after application of isoproterenol (10 nmol/L) and following subsequent application of ANP or mANP in the presence of isoproterenol (Figure 7A). These activation maps demonstrate that the first electric breakthrough occurs in the right atrial posterior wall, which corresponds to the location of the sinoatrial node,¹⁷ and that conduction propagates from this site into the right and left atrial appendages. As expected, isoproterenol sped conduction time throughout the atrial preparation (fewer isochrones with more space between successive isochrones in the presence of isoproterenol). Application of ANP in the presence of isoproterenol further sped conduction, whereas mANP had the opposite effect and slowed electrical conduction time across the atrial preparation.

To further quantify the effects of ANP and mANP (in the presence of isoproterenol) on electrical conduction, we measured local conduction velocity (CV) in the right and left atrial appendages using a previously described approach¹⁷ (Methods). Initially, CV was measured in atrial preparations in sinus rhythm where the cycle length was free to change. Summary data demonstrate that, as expected, isoproterenol decreased ($P<0.05$) cycle length, which corresponds to an increase in heart rate. ANP further shortened ($P<0.05$) the isoproterenol-stimulated cycle length (Figure 7B). In contrast, mANP tended to increase cycle length, although this did not reach statistical significance ($P=0.09$; Figure 7B).

Analysis of atrial CV (in sinus rhythm) demonstrates that isoproterenol increased ($P<0.05$) CV in the right and left atria and that subsequent application of ANP in the presence of isoproterenol further increased ($P<0.05$) right atrial and left atrial CVs (Figure 7C). These changes in CV are consistent with the effects of isoproterenol and ANP on atrial AP V_{max} (Figure 1), which is a key determinant of CV in the heart.³⁶ Once again, mANP had the opposite effects to ANP and decreased ($P<0.05$) CV in the right and left atria (Figure 7D). This is in agreement with the finding that mANP also decreased V_{max} (Figure 2) in isolated atrial myocytes. To account for the possibility of rate-dependent effects, we also measured right and left atrial CV in atrial preparations paced at a fixed cycle length of 90 ms (Figure 7E and 7F). These data demonstrate similar effects of ANP and mANP on atrial CV to those observed in sinus rhythm.

Our optical mapping studies also enabled us to assess changes in APD in the intact atrial preparation by measuring optical APs (Figure XI in the Data Supplement). Optical APs were measured in the right atrial myocardium after application of isoproterenol (10 nmol/L) and then ANP or mANP (50 nmol/L each). Isoproterenol increased ($P<0.05$) APD₇₀ in atrial preparations, and consistent with our studies in isolated myocytes, subsequent application of ANP further increased APD₇₀ ($P<0.05$), whereas mANP decreased isoproterenol-stimulated APD₇₀.

Because changes in APD are known to affect atrial ERP, we used programmed stimulation to measure the effects of isoproterenol, ANP, and mANP on ERP in isolated atrial preparations (Figure XI in the Data Supplement). Consistent with increases in APD in isolated myocytes and intact atrial preparations, isoproterenol (10 nmol/L) increased ($P<0.05$) atrial ERP. Once again, ANP (50 nmol/L) and mANP (50 nmol/L) had opposite effects on refractoriness whereby ANP increased ($P<0.05$) atrial ERP and mANP decreased ($P<0.05$) atrial ERP.

Effects of ANP and mANP on Arrhythmogenesis

Finally, we used high-resolution optical mapping in conjunction with atrial pacing/programmed stimulation to study the effects of ANP and mANP on inducibility of arrhythmias in mouse atrial preparations. These pacing studies were performed in atrial preparations in the presence of isoproterenol (10 nmol/L) and either ANP (50 nmol/L) or mANP (50 nmol/L) to mimic the conditions in which the 2 peptides elicited opposing effects on atrial conduction and ERP. Figure 8A and 8B illustrate activation maps before and after atrial pacing in the presence of isoproterenol and ANP. These images demonstrate that the heart was in sinus rhythm and activation patterns were normal (ie, conduction initiated in the right atrial posterior wall and then propagated uniformly throughout the atrial preparation) before and after pacing.

Figure 8C illustrates a representative activation map in the presence of isoproterenol and mANP before pacing. This map demonstrates a normal conduction pattern although, consistent with the data in Figure 7, conduction was slowed in the presence of mANP compared with ANP. Strikingly, atrial pacing in the presence of mANP resulted in the induction of atrial arrhythmias (Figure 8D). Specifically, delivery of premature stimuli resulted in the occurrence of multiple points of simultaneous activation (red color) including ectopic foci in the right atrium near the pectinate muscles. These ectopic foci were associated with a re-entrant pattern of conduction (white arrow in Figure 8D) in the right atrium. In this example, we also observed conduction to the left atrium via an activation point in the right atrial posterior wall that was similar to the normal initial activation point before pacing (black arrow in Figure 8D); however, conduction to the right atrial appendage from the normal excitation point was blocked. In other instances, we observed similar re-entrant patterns of conduction in the right atrium with no propagation to the left atrium (not shown). Summary data (Figure 8E) demonstrate that in the presence of isoproterenol and ANP, all atrial preparations remained in normal sinus rhythm and no arrhythmias were induced after atrial pacing in these conditions. In contrast, we

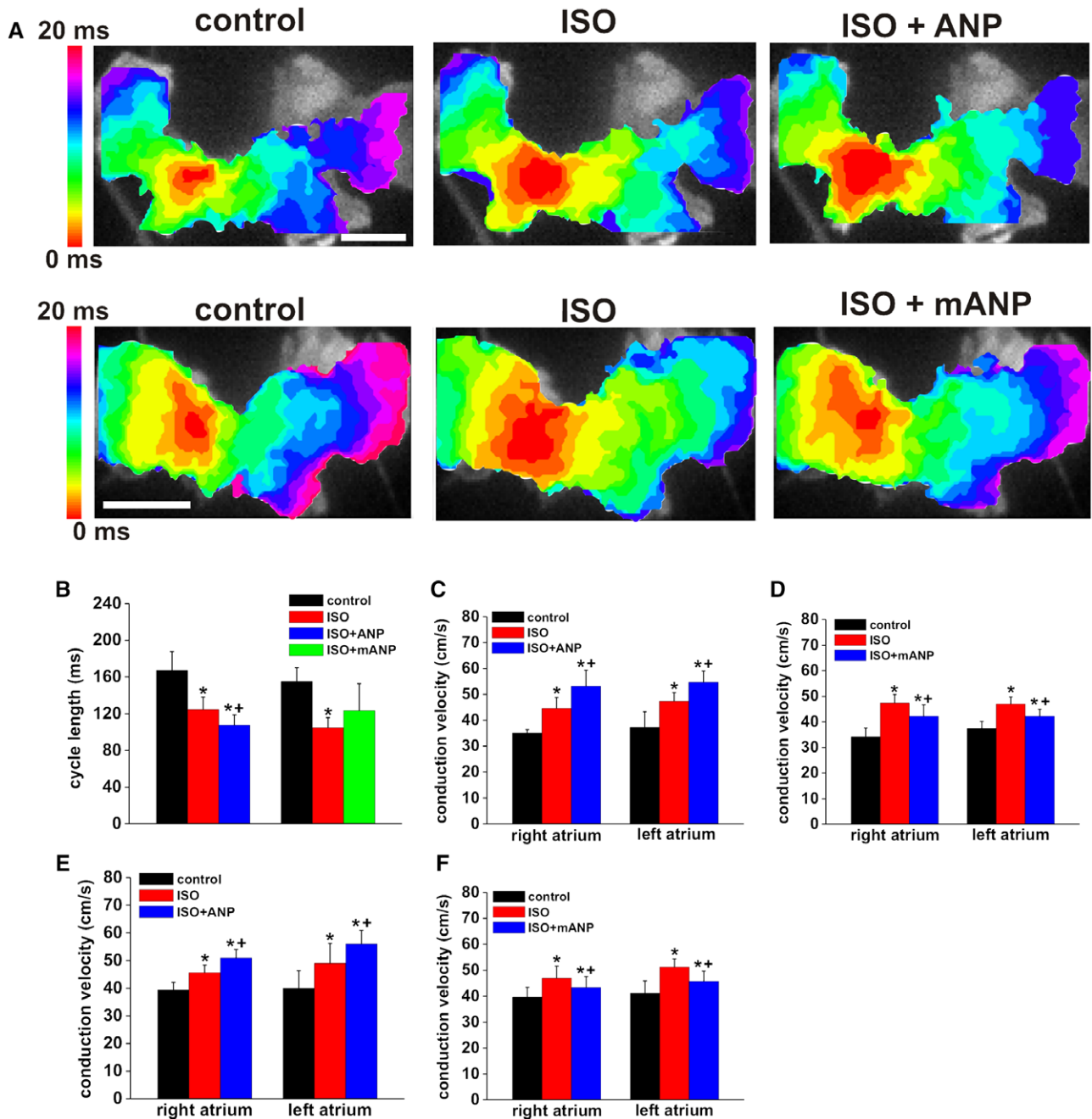


Figure 7. Atrial natriuretic peptide (ANP) and mutant ANP (mANP) have opposing effects on electrical conduction in the atria in mice. **A**, Representative color maps showing activation patterns in atrial preparations (Figure X in the Data Supplement) in control conditions, in the presence of isoproterenol (ISO; 10 nmol/L), and after application of ANP (50 nmol/L; **top**) or mANP (50 nmol/L; **bottom**). Scale bar, 2 mm. The right atrial appendage is on the left side of the image and the red color indicates the earliest activation time in the right atrial posterior wall. Time interval between isochrones is 1 ms. **B**, Summary of the effects of ANP and mANP on cycle length in atrial preparations in sinus rhythm. **C** and **D**, Summary data illustrating the effects of ANP and mANP on right and left atrial conduction velocities in atrial preparations in sinus rhythm (n=5 hearts for each condition). **E** and **F**, Summary data illustrating the effects of ANP and mANP on right and left atrial conduction velocities in atrial preparations paced a fixed cycle length of 90 ms. * $P < 0.05$ vs control; + $P < 0.05$ vs ISO by 1-way repeated measures ANOVA with Tukey post hoc test; n=8 hearts for each condition.

observed arrhythmias in 62.5% of hearts (5/8 hearts; $P < 0.05$) after atrial pacing in the presence of isoproterenol and mANP. In all cases, these arrhythmias were characterized by disorganized activation patterns, re-entrant conduction patterns, and multiple ectopic foci similar to those shown in Figure 8. Thus, mANP-treated hearts were highly susceptible to induced arrhythmias, whereas hearts treated with ANP were protected.

Discussion

In this study, we have used mouse and human tissues to compare the effects of wild-type ANP and mANP (which has been associated with AF in the human population). Previous work that measured monophasic APs in rat hearts demonstrated that mANP could decrease APD.¹¹ Furthermore, the human patients affected by this mutation had circulating levels of mANP that

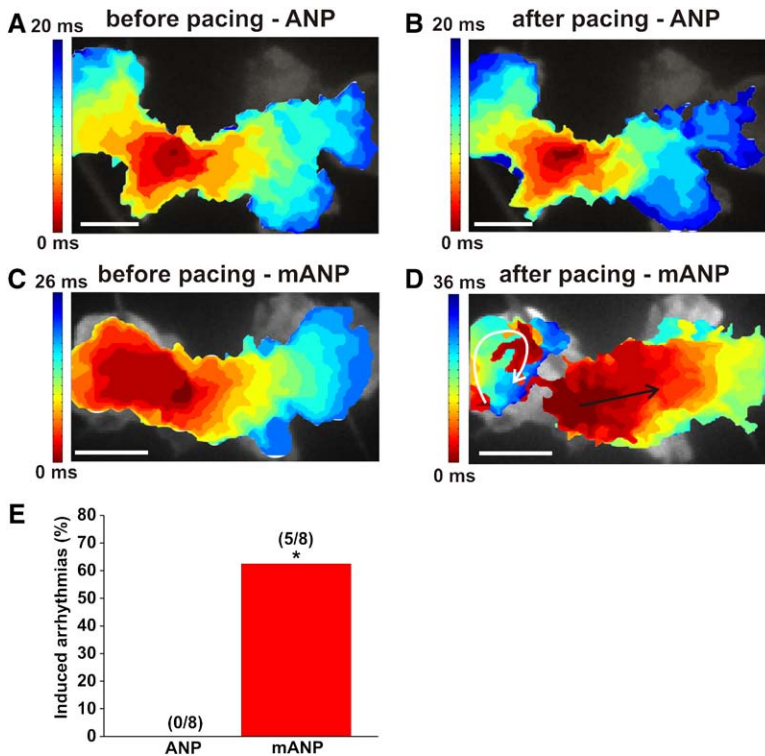


Figure 8. Effects of atrial natriuretic peptide (ANP) and mutant ANP (mANP) on susceptibility to arrhythmias during atrial pacing. These experiments were performed in atrial preparations in the presence of isoproterenol (ISO; 10 nmol/L) and either ANP (50 nmol/L) or mANP (50 nmol/L). Arrhythmias were induced using S1–S2 protocols in which atrial preparations were paced a fixed cycle length (90 ms) and then given a series of premature extra stimuli (Methods). **A** and **B**, Representative color maps from before and after atrial pacing in the presence of ISO and ANP. These activation maps show that after pacing, atrial preparations treated with ANP remained in sinus rhythm (**B**) with activation patterns similar to those before pacing (**A**). **C** and **D**, Representative color maps from before and after atrial pacing in the presence of ISO and mANP. In these examples, the atrial preparation is in normal sinus rhythm before atrial pacing has occurred (**C**). After pacing in the presence of mANP (**D**), electrical conduction became arrhythmic. Note the different time scales in these activation maps. Time interval between isochrones is 1 ms in all maps; scale bar, 2 mm. **E**, Summary of the susceptibility to arrhythmias in atrial preparations treated with ANP or mANP (both in the presence of ISO). Numbers in parentheses indicate the number of hearts that showed arrhythmias; **P*<0.05 vs ANP by Fisher exact test.

were 5 to 10× greater than those of wild-type ANP.¹¹ Subsequent biochemical studies showed that mANP was much more resistant to proteolytic degradation, which likely explains the elevated circulating levels of this mutant peptide compared with normal ANP.²⁷ These findings led to the hypothesis that mANP functions similarly to ANP but with enhanced effects because of the profound elevation in plasma concentrations of the peptide and that this could predispose these patients to AF. Although the high circulating levels of mANP may contribute to its proarrhythmic actions, the specific electrophysiological effects of mANP and the mechanism(s) through which it elicits its effects have not been previously studied.

We studied the effects of ANP and mANP using identical doses (1–100 nmol/L) to determine whether mANP has unique effects on atrial electrophysiology independently of differences in plasma concentration. Surprisingly, we found that ANP and mANP had distinct and opposing effects on atrial electrophysiology (including V_{max} , APD, I_{CaL} , CV, and ERP). The stimulatory effects of ANP and the inhibitory effects of mANP on I_{CaL} were found to be similar in right and left atrial myocytes from mice. When ANP and mANP were applied concomitantly at identical doses, we observed no effect on atrial electrophysiology, indicating that the peptides negated each other’s effects. Our mechanistic experiments using NPR-C^{-/-} mice and an NPR-A antagonist conclusively demonstrate that ANP affects atrial electrophysiology via the NPR-A receptor, whereas mANP signals via NPR-C.

These novel findings strongly suggest that mANP may be proarrhythmic not only because it circulates at a higher concentration than ANP but also because it elicits electrophysiological effects that are distinct from those of ANP (ie, mANP is not simply enhancing the effects of ANP in a concentration-dependent manner). Because the circulating concentration

of mANP was so much higher than that of ANP in individuals affected by this mutation, it is possible that the effects of mANP may be more robust than those of ANP and that the effects of mANP may dominate in vivo. We also found that the expression of NPR-C, which mediates the effects of mANP, is much higher in human atria than that of NPR-A, which may further enhance the effects of mANP compared with ANP.

Many of the effects of NPs on the heart are dose dependent.^{13,14,17} Our electrophysiological studies demonstrate that the effects of ANP and mANP on atrial electrophysiology are comparable at doses from 10 to 100 nmol/L and smaller, but still significant, at doses as low as 1 nmol/L. Although some of these doses of ANP are higher than typical circulating levels,¹⁰ it is possible that mANP, because of its enhanced resistance to proteolytic degradation,²⁷ could achieve low nanomolar concentrations in the circulation, particularly in conditions where atrial stretch is enhanced and NP production is increased. Furthermore, it is important to note that because ANP (and mANP) are produced in atrial myocytes, the local concentrations of these peptides in the atria are likely to be much higher than circulating concentrations. All of these factors suggest that the effects of ANP and mANP we have described at low nanomolar concentrations are physiologically relevant.

Interestingly, although we observed clear effects of isoproterenol, ANP, and mANP on V_{max} and atrial CV, we found no direct effects of any of these compounds on atrial I_{Na} . This was surprising because I_{Na} is the main determinant of V_{max} , which in turn contributes importantly to CV.³⁶ Furthermore, we showed that the electrophysiological effects of ANP and mANP are associated with changes in cAMP production. Several studies have shown that cAMP and protein kinase A can directly modulate voltage-gated sodium channels,^{37–39} although not all studies agree on this.^{40,41} The lack of direct effects of ANP and

mANP on atrial I_{Na} in our study suggests that ANP and mANP are modulating V_{max} and atrial CV via their robust effects on $I_{Ca,L}$. Consistent with this hypothesis, changes in calcium are known to have potent effects on V_{max} ⁴² and calcium is known to regulate sodium channels.^{43–45} Thus, ANP and mANP could modulate I_{Na} secondary to changes in $I_{Ca,L}$. In our I_{Na} recordings, $I_{Ca,L}$ is blocked and Ca^{2+} transients are suppressed, which could explain why we did not observe any effects of ANP/mANP on I_{Na} in our experimental conditions.

It is also possible that changes in $I_{Ca,L}$ could directly contribute to changes in V_{max} and CV as $I_{Ca,L}$ is known to have effects on electrical conduction in some conditions.³⁶ Although these effects are smaller than those exerted by I_{Na} , they may be important in the atrial myocardium because of the expression of $Ca_v1.3$ L-type Ca^{2+} channels in this region of the heart.^{46,47} $Ca_v1.3$ -mediated $I_{Ca,L}$ activates at more negative membrane potentials than $Ca_v1.2$,⁴⁶ which could result in a greater contribution by $I_{Ca,L}$ to the AP upstroke in the atrial myocardium. Our $I_{Ca,L}$ recordings were done using a voltage clamp protocol that measures total $I_{Ca,L}$ ($Ca_v1.2$ and $Ca_v1.3$ dependent). The left shifts in $I_{Ca,L}$ $V_{1/2(act)}$ elicited by isoproterenol and ANP could result in a greater influence of $I_{Ca,L}$ on V_{max} in atrial myocytes and contribute to the increases in V_{max} we observed. In contrast, the right shift in $I_{Ca,L}$ $V_{1/2(act)}$ elicited by mANP could reduce V_{max} . $Ca_v1.2$ and $Ca_v1.3$ are both known to be regulated by cAMP and protein kinase A^{48–50}; therefore, we anticipate that both channels are being similarly modulated by isoproterenol, ANP, and mANP; however, we have not studied each channel separately in this study.

Electrical re-entry is thought to be a major factor in AF with the wavelength of re-entry being determined by the product of the atrial ERP and atrial CV.^{4,33,51,52} Reductions in wavelength that favor the occurrence of AF are commonly associated with changes in ion-channel function or regulation in atrial myocytes.^{53–55} Our novel studies demonstrate that mANP decreases APD (which corresponds to a reduction in atrial refractory period) and V_{max} (which is consistent with the slowing of atrial CV). In agreement with these findings, direct assessment of refractoriness in intact atrial preparations illustrates that mANP shortened atrial ERP. These effects on CV and ERP would be expected to decrease the wavelength of re-entry and could explain how mANP leads to the occurrence of AF. In contrast, and consistent with our previous studies of the effects of BNP and CNP on atrial electrophysiology,^{13,14,17} our experiments show that wild-type ANP increases APD and V_{max} , speeds electric conduction in both the right and left atria, and increases atrial ERP. These effects would increase the wavelength of re-entry and would be expected to decrease the likelihood of AF, suggesting that wild-type ANP could be antiarrhythmic. Consistent with these concepts, we found that mANP greatly increased the susceptibility to arrhythmias during pacing studies in atrial preparations. These arrhythmias were characterized by re-entrant conduction patterns, ectopic foci of activation, and conduction block, all of which are associated with atrial flutter and AF.^{56–58} In agreement with a key role for $I_{Ca,L}$ in the occurrence of atrial arrhythmias in the presence of mANP, reductions in both $Ca_v1.2$ and $Ca_v1.3$ expression or function are known to profoundly increase susceptibility to AF in animal models and humans.^{47,58–61}

This study indicates that changes in cAMP are central to the electrophysiological effects of wild-type NPs, as well as mANP, in the heart. Effects mediated by the NPR-A receptor involve a cyclic GMP-mediated inhibition of PDE3, which would lead to elevated cAMP levels, whereas effects mediated by NPR-C involve the inhibition of adenylyl cyclase and reductions in cAMP. Importantly, this study shows that the electrophysiological effects of ANP and mANP were only evident in the mouse in the presence of isoproterenol. This is in agreement with the observations that neither ANP nor mANP had any effects on cAMP production in the absence of isoproterenol in mouse atrial myocytes and further supports the conclusion that the electrophysiological effects of ANP and mANP are associated with changes in cAMP signaling. Changes in cAMP concentration are known to affect $I_{Ca,L}$ via changes in phosphorylation of L-type Ca^{2+} channels by protein kinase A, which shifts the voltage dependence of activation and increases the channel open probability.⁶² Our biophysical analyses showing that the effects of both ANP and mANP on atrial $I_{Ca,L}$ are associated with shifts in the $V_{1/2}$ of channel activation strongly suggest that these peptides cause cAMP-dependent changes in protein kinase A phosphorylation of L-type Ca^{2+} channels.

Our study demonstrates that the distinct effects of ANP and mANP on $I_{Ca,L}$ are also present in human atrial myocytes with some minor differences compared with the mouse. Specifically, in mice, ANP only increased atrial $I_{Ca,L}$ in the presence of isoproterenol, whereas in humans, ANP potently increased atrial $I_{Ca,L}$ in basal conditions and in the presence of isoproterenol. This is because the stimulatory effect of NPs on atrial $I_{Ca,L}$ (mediated by NPR-A) occurs via the inhibition of PDE3.¹³ We have previously shown that mouse atrial myocytes lack constitutive PDE3 activity,³² which is why NPs, including ANP, have no effect on basal atrial electrophysiology in mice.¹³ In contrast, this study shows that human atrial myocytes have robust constitutive PDE3 activity, and this explains why ANP can modulate human $I_{Ca,L}$ in basal conditions. Our observation that human atrial myocytes have constitutive PDE3 activity is consistent with previous studies showing similar results.^{63,64} The inhibitory effects of mANP on atrial $I_{Ca,L}$ were similar in mice and humans and were only observed in the presence of isoproterenol. This is highly consistent with our previous studies demonstrating that NPR-C-mediated effects of NPs on cardiac electrophysiology are most prominent in the setting of β -adrenergic receptor activation.^{13,14,16,17} All of our human $I_{Ca,L}$ measurements were performed in right atrial myocytes. On the basis of our data showing that the effects of ANP and mANP are similar in right and left atrial myocytes in mice, we hypothesize that this is the case in the human heart as well; however, we have not directly measured the effects of NPs in human left atrial myocytes.

The similarities between the electrophysiological effects of ANP and mANP in mice and humans (particularly in the presence of isoproterenol) strongly suggest a mechanism for how mANP causes AF in humans. Nevertheless, extrapolation of our mouse arrhythmogenesis studies to humans must be done with some caution as our results do demonstrate some differences in PDE3 activity and how $I_{Ca,L}$ is regulated by NPs in mice and humans. Clearly, additional studies in humans are warranted.

Although our study provides novel insight into how mANP could create a substrate for AF, our experiments also demonstrate that wild-type ANP is protective against atrial arrhythmias, possibly in association with its AP lengthening and CV speeding effects. These effects of ANP would be expected to increase the wavelength of re-entry and decrease the likelihood of AF being initiated. The antiarrhythmic effects of wild-type ANP have not been well studied; however, there is evidence that ANP can reduce the incidence of postoperative AF during cardiothoracic surgeries.^{65–67} To better appreciate the role of wild-type ANP in human AF, it will be important to study the electrophysiological effects of ANP in atrial myocytes from human patients with a history of AF. AF is associated with electrical remodeling, including alterations in Ca²⁺-channel expression,⁵⁹ which may affect the effects of ANP on I_{CaL} in this setting. For example, it has recently been shown that the effects of nitric oxide on atrial I_{CaL} are attenuated and distinct, whereas the responsiveness to isoproterenol is preserved, in atrial myocytes isolated from patients with chronic AF.⁶⁴ It is presently unknown how chronic AF affects the electrophysiological effects of ANP.

In conclusion, we have studied the effects of ANP and mANP on atrial electrophysiology in mice and humans. Our study provides new insight into the unique electrophysiological effects of mANP and suggests that this mutation promotes AF by decreasing AP V_{max} , shortening atrial APD, decreasing I_{CaL} , and slowing atrial CV. In contrast, wild-type ANP has the opposite effects, which would be expected to decrease the susceptibility to AF by increasing the wavelength of re-entry, although additional studies are required to fully assess the effect of differences between mouse and human atrial electrophysiology. These findings advance our understanding of the electrophysiological effects of wild-type and mutated NPs in the heart and suggest that the NP system could be a target for treating or preventing AF.

Acknowledgments

We sincerely thank Sara Rafferty for outstanding technical assistance.

Sources of Funding

This work was supported by operating grants from the Heart and Stroke Foundation of Nova Scotia and The Canadian Institutes of Health Research (CIHR; MOP 93718) to R.A. Rose who holds New Investigator Awards from the CIHR and the Heart and Stroke Foundation of Canada. R. Hua is the recipient of a Heart and Stroke Foundation Fellowship award.

Disclosures

None.

References

- Dobrev D, Nattel S. New antiarrhythmic drugs for treatment of atrial fibrillation. *Lancet*. 2010;375:1212–1223. doi: 10.1016/S0140-6736(10)60096-7.
- McManus DD, Rienstra M, Benjamin EJ. An update on the prognosis of patients with atrial fibrillation. *Circulation*. 2012;126:e143–e146. doi: 10.1161/CIRCULATIONAHA.112.129759.
- Nattel S, Opie LH. Controversies in atrial fibrillation. *Lancet*. 2006;367:262–272. doi: 10.1016/S0140-6736(06)68037-9.
- Nattel S. New ideas about atrial fibrillation 50 years on. *Nature*. 2002;415:219–226. doi: 10.1038/415219a.
- Kopecky SL, Gersh BJ, McGoon MD, Whisnant JP, Holmes DR Jr, Ilstrup DM, Frye RL. The natural history of lone atrial fibrillation. A population-based study over three decades. *N Engl J Med*. 1987;317:669–674. doi: 10.1056/NEJM198709103171104.
- Chen YH, Xu SJ, Bendahhou S, Wang XL, Wang Y, Xu WY, Jin HW, Sun H, Su XY, Zhuang QN, Yang YQ, Li YB, Liu Y, Xu HJ, Li XF, Ma N, Mou CP, Chen Z, Barhanin J, Huang W. KCNQ1 gain-of-function mutation in familial atrial fibrillation. *Science*. 2003;299:251–254. doi: 10.1126/science.1077771.
- Olson TM, Alekseev AE, Liu XK, Park S, Zingman LV, Bienengraeber M, Sattiraju S, Ballew JD, Jahangir A, Terzic A. Kv1.5 channelopathy due to KCNA5 loss-of-function mutation causes human atrial fibrillation. *Hum Mol Genet*. 2006;15:2185–2191. doi: 10.1093/hmg/ddl143.
- Olson TM, Michels VV, Ballew JD, Reyna SP, Karst ML, Herron KJ, Horton SC, Rodeheffer RJ, Anderson JL. Sodium channel mutations and susceptibility to heart failure and atrial fibrillation. *JAMA*. 2005;293:447–454. doi: 10.1001/jama.293.4.447.
- Gollob MH, Jones DL, Krahn AD, Danis L, Gong XQ, Shao Q, Liu X, Veinot JP, Tang AS, Stewart AF, Tesson F, Klein GJ, Yee R, Skanes AC, Guiraudon GM, Ebihara L, Bai D. Somatic mutations in the connexin 40 gene (GJA5) in atrial fibrillation. *N Engl J Med*. 2006;354:2677–2688. doi: 10.1056/NEJMoa052800.
- Potter LR, Abbey-Hosch S, Dickey DM. Natriuretic peptides, their receptors, and cyclic guanosine monophosphate-dependent signaling functions. *Endocr Rev*. 2006;27:47–72. doi: 10.1210/er.2005-0014.
- Hodgson-Zingman DM, Karst ML, Zingman LV, Heublein DM, Darbar D, Herron KJ, Ballew JD, de Andrade M, Burnett JC Jr, Olson TM. Atrial natriuretic peptide frameshift mutation in familial atrial fibrillation. *N Engl J Med*. 2008;359:158–165. doi: 10.1056/NEJMoa0706300.
- Levin ER, Gardner DG, Samson WK. Natriuretic peptides. *N Engl J Med*. 1998;339:321–328. doi: 10.1056/NEJM199807033390507.
- Springer J, Azer J, Hua R, Robbins C, Adamczyk A, McBoyle S, Bissell MB, Rose RA. The natriuretic peptides BNP and CNP increase heart rate and electrical conduction by stimulating ionic currents in the sinoatrial node and atrial myocardium following activation of guanylyl cyclase-linked natriuretic peptide receptors. *J Mol Cell Cardiol*. 2012;52:1122–1134. doi: 10.1016/j.yjmcc.2012.01.018.
- Azer J, Hua R, Vella K, Rose RA. Natriuretic peptides regulate heart rate and sinoatrial node function by activating multiple natriuretic peptide receptors. *J Mol Cell Cardiol*. 2012;53:715–724. doi: 10.1016/j.yjmcc.2012.08.020.
- Rose RA, Lomax AE, Giles WR. Inhibition of L-type Ca²⁺ current by C-type natriuretic peptide in bullfrog atrial myocytes: an NPR-C-mediated effect. *Am J Physiol Heart Circ Physiol*. 2003;285:H2454–H2462. doi: 10.1152/ajpheart.00388.2003.
- Rose RA, Lomax AE, Kondo CS, Anand-Srivastava MB, Giles WR. Effects of C-type natriuretic peptide on ionic currents in mouse sinoatrial node: a role for the NPR-C receptor. *Am J Physiol Heart Circ Physiol*. 2004;286:H1970–H1977. doi: 10.1152/ajpheart.00893.2003.
- Azer J, Hua R, Krishnaswamy PS, Rose RA. Effects of natriuretic peptides on electrical conduction in the sinoatrial node and atrial myocardium of the heart. *J Physiol*. 2014;592(Pt 5):1025–1045. doi: 10.1113/jphysiol.2013.265405.
- Anand-Srivastava MB, Trachte GJ. Atrial natriuretic factor receptors and signal transduction mechanisms. *Pharmacol Rev*. 1993;45:455–497.
- Kuhn M. Molecular physiology of natriuretic peptide signalling. *Basic Res Cardiol*. 2004;99:76–82. doi: 10.1007/s00395-004-0460-0.
- Lucas KA, Pitari GM, Kazerounian S, Ruiz-Stewart I, Park J, Schulz S, Chepenik KP, Waldman SA. Guanylyl cyclases and signaling by cyclic GMP. *Pharmacol Rev*. 2000;52:375–414.
- Anand-Srivastava MB. Natriuretic peptide receptor-C signaling and regulation. *Peptides*. 2005;26:1044–1059. doi: 10.1016/j.peptides.2004.09.023.
- Rose RA, Giles WR. Natriuretic peptide C receptor signalling in the heart and vasculature. *J Physiol*. 2008;586:353–366. doi: 10.1113/jphysiol.2007.144253.
- Pagano M, Anand-Srivastava MB. Cytoplasmic domain of natriuretic peptide receptor C constitutes Gi activator sequences that inhibit adenylyl cyclase activity. *J Biol Chem*. 2001;276:22064–22070. doi: 10.1074/jbc.M101587200.
- Zhou H, Murthy KS. Identification of the G protein-activating sequence of the single-transmembrane natriuretic peptide receptor C (NPR-C). *Am J Physiol Cell Physiol*. 2003;284:C1255–C1261. doi: 10.1152/ajpcell.00520.2002.
- Perrin MJ, Gollob MH. The role of atrial natriuretic peptide in modulating cardiac electrophysiology. *Heart Rhythm*. 2012;9:610–615. doi: 10.1016/j.hrthm.2011.11.019.
- Jaubert J, Jaubert F, Martin N, Washburn LL, Lee BK, Eicher EM, Guénet JL. Three new allelic mouse mutations that cause skeletal overgrowth involve the natriuretic peptide receptor C gene (Npr3). *Proc Natl Acad Sci U S A*. 1999;96:10278–10283.

27. Dickey DM, Yoder AR, Potter LR. A familial mutation renders atrial natriuretic Peptide resistant to proteolytic degradation. *J Biol Chem*. 2009;284:19196–19202. doi: 10.1074/jbc.M109.010777.
28. Egom EE, Vella K, Hua R, Jansen HJ, Moghtadaei M, Polina I, Bogachev O, Humnik R, Mackasey M, Rafferty S, Ray G, Rose RA. Impaired sinoatrial node function and increased susceptibility to atrial fibrillation in mice lacking natriuretic peptide receptor C. *J Physiol*. 2015;593:1127–1146. doi: 10.1113/jphysiol.2014.283135.
29. Krishnaswamy PS, Egom EE, Moghtadaei M, Jansen HJ, Azer J, Bogachev O, Mackasey M, Robbins C, Rose RA. Altered parasympathetic nervous system regulation of the sinoatrial node in Akita diabetic mice. *J Mol Cell Cardiol*. 2015;82:125–135. doi: 10.1016/j.yjmcc.2015.02.024.
30. Delporte C, Winand J, Poloczek P, Von Geldern T, Christophe J. Discovery of a potent atrial natriuretic peptide antagonist for ANPA receptors in the human neuroblastoma NB-OK-1 cell line. *Eur J Pharmacol*. 1992;224:183–188.
31. Anand-Srivastava MB, Sehl PD, Lowe DG. Cytoplasmic domain of natriuretic peptide receptor-C inhibits adenylyl cyclase. Involvement of a pertussis toxin-sensitive G protein. *J Biol Chem*. 1996;271:19324–19329.
32. Hua R, Adamczyk A, Robbins C, Ray G, Rose RA. Distinct patterns of constitutive phosphodiesterase activity in mouse sinoatrial node and atrial myocardium. *PLoS One*. 2012;7:e47652. doi: 10.1371/journal.pone.0047652.
33. Jalife J, Berenfeld O, Mansour M. Mother rotors and fibrillatory conduction: a mechanism of atrial fibrillation. *Cardiovasc Res*. 2002;54:204–216.
34. Nygren A, Lomax AE, Giles WR. Heterogeneity of action potential durations in isolated mouse left and right atria recorded using voltage-sensitive dye mapping. *Am J Physiol Heart Circ Physiol*. 2004;287:H2634–H2643. doi: 10.1152/ajpheart.00380.2004.
35. Glukhov AV, Fedorov VV, Anderson ME, Mohler PJ, Efimov IR. Functional anatomy of the murine sinus node: high-resolution optical mapping of ankyrin-B heterozygous mice. *Am J Physiol Heart Circ Physiol*. 2010;299:H482–H491. doi: 10.1152/ajpheart.00756.2009.
36. Kléber AG, Rudy Y. Basic mechanisms of cardiac impulse propagation and associated arrhythmias. *Physiol Rev*. 2004;84:431–488. doi: 10.1152/physrev.00025.2003.
37. Yarbrough TL, Lu T, Lee HC, Shibata EF. Localization of cardiac sodium channels in caveolin-rich membrane domains: regulation of sodium current amplitude. *Circ Res*. 2002;90:443–449.
38. Matsuda JJ, Lee H, Shibata EF. Enhancement of rabbit cardiac sodium channels by beta-adrenergic stimulation. *Circ Res*. 1992;70:199–207.
39. Lu T, Lee HC, Kabat JA, Shibata EF. Modulation of rat cardiac sodium channel by the stimulatory G protein alpha subunit. *J Physiol*. 1999;518(Pt 2):371–384.
40. Abriel H. Roles and regulation of the cardiac sodium channel Na v 1.5: recent insights from experimental studies. *Cardiovasc Res*. 2007;76:381–389. doi: 10.1016/j.cardiores.2007.07.019.
41. Ono K, Kiyosue T, Arita M. Isoproterenol, DBcAMP, and forskolin inhibit cardiac sodium current. *Am J Physiol*. 1989;256(6 Pt 1):C1131–C1137.
42. Weidmann S. Effects of calcium ions and local anesthetics on electrical properties of Purkinje fibres. *J Physiol*. 1955;129:568–582.
43. Shah VN, Wingo TL, Weiss KL, Williams CK, Balsler JR, Chazin WJ. Calcium-dependent regulation of the voltage-gated sodium channel hH1: intrinsic and extrinsic sensors use a common molecular switch. *Proc Natl Acad Sci U S A*. 2006;103:3592–3597. doi: 10.1073/pnas.0507397103.
44. Wingo TL, Shah VN, Anderson ME, Lybrand TP, Chazin WJ, Balsler JR. An EF-hand in the sodium channel couples intracellular calcium to cardiac excitability. *Nat Struct Mol Biol*. 2004;11:219–225. doi: 10.1038/nsmb737.
45. Mori M, Konno T, Ozawa T, Murata M, Imoto K, Nagayama K. Novel interaction of the voltage-dependent sodium channel (VDSC) with calmodulin: does VDSC acquire calmodulin-mediated Ca²⁺-sensitivity? *Biochemistry*. 2000;39:1316–1323.
46. Mangoni ME, Couette B, Bourinet E, Platzer J, Reimer D, Striessnig J, Nargeot J. Functional role of L-type Cav1.3 Ca²⁺ channels in cardiac pacemaker activity. *Proc Natl Acad Sci U S A*. 2003;100:5543–5548. doi: 10.1073/pnas.0935295100.
47. Zhang Z, He Y, Tuteja D, Xu D, Timofeyev V, Zhang Q, Glatter KA, Xu Y, Shin HS, Low R, Chiamvimonvat N. Functional roles of Cav1.3(alpha1D) calcium channels in atria: insights gained from gene-targeted null mutant mice. *Circulation*. 2005;112:1936–1944. doi: 10.1161/CIRCULATIONAHA.105.540070.
48. Qu Y, Baroudi G, Yue Y, El-Sherif N, Boutjdir M. Localization and modulation of {alpha}1D (Cav1.3) L-type Ca channel by protein kinase A. *Am J Physiol Heart Circ Physiol*. 2005;288:H2123–H2130. doi: 10.1152/ajpheart.01023.2004.
49. Vandael DH, Mahapatra S, Calorio C, Marcantoni A, Carbone E. Cav1.3 and Cav1.2 channels of adrenal chromaffin cells: emerging views on cAMP/cGMP-mediated phosphorylation and role in pacemaking. *Biochim Biophys Acta*. 2013;1828:1608–1618. doi: 10.1016/j.bbame.2012.11.013.
50. Striessnig J, Pinggera A, Kaur G, Bock G, Tuluc P. L-type Ca(2+) channels in heart and brain. *Wiley Interdiscip Rev Membr Transp Signal*. 2014;3:15–38. doi: 10.1002/wmts.102.
51. Pandit SV, Jalife J. Rotors and the dynamics of cardiac fibrillation. *Circ Res*. 2013;112:849–862. doi: 10.1161/CIRCRESAHA.111.300158.
52. Allesie MA, Bonke FI, Schopman FJ. Circus movement in rabbit atrial muscle as a mechanism of tachycardia. III. The “leading circle” concept: a new model of circus movement in cardiac tissue without the involvement of an anatomical obstacle. *Circ Res*. 1977;41:9–18.
53. Greiser M, Lederer WJ, Schotten U. Alterations of atrial Ca(2+) handling as cause and consequence of atrial fibrillation. *Cardiovasc Res*. 2011;89:722–733. doi: 10.1093/cvr/cvq389.
54. Nattel S, Harada M. Atrial remodeling and atrial fibrillation: recent advances and translational perspectives. *J Am Coll Cardiol*. 2014;63:2335–2345. doi: 10.1016/j.jacc.2014.02.555.
55. Wolf RM, Glynn P, Hashemi S, Zarei K, Mitchell CC, Anderson ME, Mohler PJ, Hund TJ. Atrial fibrillation and sinus node dysfunction in human ankyrin-B syndrome: a computational analysis. *Am J Physiol Heart Circ Physiol*. 2013;304:H1253–H1266. doi: 10.1152/ajpheart.00734.2012.
56. Fedorov VV, Chang R, Glukhov AV, Kostecky G, Janks D, Schuessler RB, Efimov IR. Complex interactions between the sinoatrial node and atrium during reentrant arrhythmias in the canine heart. *Circulation*. 2010;122:782–789. doi: 10.1161/CIRCULATIONAHA.109.935288.
57. Choi EK, Chang PC, Lee YS, Lin SF, Zhu W, Maruyama M, Fishbein MC, Chen Z, Rubart-von der Lohe M, Field LJ, Chen PS. Triggered firing and atrial fibrillation in transgenic mice with selective atrial fibrosis induced by overexpression of TGF-β1. *Circ J*. 2012;76:1354–1362.
58. Rose RA, Sellan M, Simpson JA, Izaddoustdar F, Cifelli C, Panama BK, Davis M, Zhao D, Markhani M, Murphy GG, Striessnig J, Liu PP, Heximer SP, Backx PH. Iron overload decreases Cav1.3-dependent L-type Ca²⁺ currents leading to bradycardia, altered electrical conduction, and atrial fibrillation. *Circ Arrhythm Electrophysiol*. 2011;4:733–742. doi: 10.1161/CIRCEP.110.960401.
59. Van Wagoner DR, Pond AL, Lamorgese M, Rossie SS, McCarthy PM, Nerbonne JM. Atrial L-type Ca²⁺ currents and human atrial fibrillation. *Circ Res*. 1999;85:428–436.
60. Yue L, Feng J, Gaspo R, Li GR, Wang Z, Nattel S. Ionic remodeling underlying action potential changes in a canine model of atrial fibrillation. *Circ Res*. 1997;81:512–525.
61. Gaborit N, Steenman M, Lamirault G, Le Meur N, Le Bouter S, Lande G, Léger J, Charpentier F, Christ T, Dobrev D, Escande D, Nattel S, Demolombe S. Human atrial ion channel and transporter subunit gene-expression remodeling associated with valvular heart disease and atrial fibrillation. *Circulation*. 2005;112:471–481. doi: 10.1161/CIRCULATIONAHA.104.506857.
62. Benitah JP, Alvarez JL, Gómez AM. L-type Ca(2+) current in ventricular cardiomyocytes. *J Mol Cell Cardiol*. 2010;48:26–36. doi: 10.1016/j.yjmcc.2009.07.026.
63. Vandecasteele G, Verde I, Rücker-Martin C, Donzeau-Gouge P, Fischmeister R. Cyclic GMP regulation of the L-type Ca(2+) channel current in human atrial myocytes. *J Physiol*. 2001;533(Pt 2):329–340.
64. Rozmaritsa N, Christ T, Van Wagoner DR, Haase H, Stasch JP, Matschke K, Ravens U. Attenuated response of L-type calcium current to nitric oxide in atrial fibrillation. *Cardiovasc Res*. 2014;101:533–542. doi: 10.1093/cvr/cvt334.
65. Sezai A, Hata M, Wakui S, Niino T, Takayama T, Hirayama A, Saito S, Minami K. Efficacy of continuous low-dose hANP administration in patients undergoing emergent coronary artery bypass grafting for acute coronary syndrome. *Circ J*. 2007;71:1401–1407.
66. Nijiri T, Yamamoto K, Maeda H, Takeuchi Y, Funakoshi Y, Inoue M, Okumura M. Effect of low-dose human atrial natriuretic peptide on postoperative atrial fibrillation in patients undergoing pulmonary resection for lung cancer: a double-blind, placebo-controlled study. *J Thorac Cardiovasc Surg*. 2012;143:488–494. doi: 10.1016/j.jtcvs.2011.09.003.
67. Sezai A, Iida M, Yoshitake I, Wakui S, Osaka S, Kimura H, Yaoita H, Hata H, Shiono M, Nakai T, Takayama T, Kunimoto S, Kasamaki Y, Hirayama A. Carperitide and atrial fibrillation after coronary bypass grafting: the Nihon University working group study of low-dose HANP infusion therapy during cardiac surgery trial for postoperative atrial fibrillation. *Circ Arrhythm Electrophysiol*. 2015;8:546–553. doi: 10.1161/CIRCEP.113.001211.

SUPPLEMENTAL MATERIAL

Methods

Animals

This study utilized male littermate wildtype (NPR-C^{+/+}) and NPR-C knockout (NPR-C^{-/-}) mice between the ages of 10-15 weeks. NPR-C^{-/-} mice were initially obtained from the Jackson Laboratory (strain B6;C-*Npr3*^{lgj/J}) and backcrossed into the C57Bl/6 line for more than 15 generations. This mouse contains a 36 base pair deletion that results in a truncated, non-functional NPR-C protein.¹

Isolation of mouse and human atrial myocytes

The procedures for isolating mouse atrial myocytes have been described previously^{2,3} and were as follows. Mice were administered a 0.2 ml intraperitoneal injection of heparin (1000 IU/ml) to prevent blood clotting. Following this, mice were anesthetized by isoflurane inhalation and then sacrificed by cervical dislocation. The heart was excised into Tyrode's solution (35°C) consisting of (in mM) 140 NaCl, 5.4 KCl, 1.2 KH₂PO₄, 1.0 MgCl₂, 1.8 CaCl₂, 5.55 glucose, and 5 HEPES, with pH adjusted to 7.4 with NaOH. The right or left atrial appendage was dissected from the heart and cut into strips, which were transferred and rinsed in a 'low Ca²⁺, Mg²⁺ free' solution containing (in mM) 140 NaCl, 5.4 KCl, 1.2 KH₂PO₄, 0.2 CaCl₂, 50 taurine, 18.5 glucose, 5 HEPES and 1 mg/ml bovine serum albumin (BSA), with pH adjusted to 6.9 with NaOH. Atrial tissue was digested in 5 ml of 'low Ca²⁺, Mg²⁺ free' solution containing collagenase (type II, Worthington Biochemical Corporation), elastase (Worthington Biochemical Corporation) and protease (type XIV, Sigma Chemical Company) for 30 min. Then the tissue was transferred to 5 ml of modified KB solution containing (in mM) 100 potassium glutamate,

10 potassium aspartate, 25 KCl, 10 KH_2PO_4 , 2 MgSO_4 , 20 taurine, 5 creatine, 0.5 EGTA, 20 glucose, 5 HEPES, and 0.1% BSA, with pH adjusted to 7.2 with KOH. The tissue was mechanically agitated using a wide-bore pipette. This procedure yielded individual right or left atrial myocytes that were stored in KB solution until experimental use within 6 hours of isolation. Mouse atrial myocytes had membrane capacitances in the range of 40 – 65 pF.

Similar procedures were used to isolate human right atrial myocytes from tissue samples obtained from cardiac surgery patients (Supplemental Table 1) with some modifications. The tissue samples were removed from patients at the time of right atrial cannulation during cardiac surgery, placed in physiological saline on ice and transported immediately to the laboratory for enzymatic digestion. Strips of human right atrial appendage were digested in the same enzyme solutions described above; however, we typically had to digest the tissue for 45-60 min. Human tissue samples were also triturated twice with a wide bore pipette – once at 30 min of digestion and again at the end of digestion. These modifications yielded individual human right atrial myocytes that were stored in KB solution until experimental use within 6 hours of isolation. Human atrial myocytes had membrane capacitances in the range of 60 – 120 pF. For human myocyte studies we ensured that at least 3 different patient samples were used for each experimental condition and/or treatment group. We also designed our study so that ANP and mANP were each measured in cells from the same patient sample. These measures were taken to account for the possibility of patient to patient variability.

Solutions and electrophysiological protocols

Stimulated action potentials (APs) were recorded using the perforated patch-clamp technique.⁴ To record APs the recording chamber was superfused with a normal Tyrode's

solution (22 – 23°C) containing (in mM) 140 NaCl, 5 KCl, 1 MgCl₂, 1 CaCl₂, 10 HEPES, and 5 glucose, with pH adjusted to 7.4 with NaOH. The pipette filling solution contained (in mM) 135 KCl, 0.1 CaCl₂, 1 MgCl₂, 5 NaCl, 10 EGTA, 4 Mg-ATP, 6.6 Na-phosphocreatine, 0.3 Na-GTP and 10 HEPES, with pH adjusted to 7.2 with KOH. Amphotericin B (200 µg/ml) was added to this pipette solution to record APs with the perforated patch clamp technique.

For recording I_{Ca,L} atrial myocytes were superfused with a modified Tyrode's solution (22 – 23°C) containing the following (in mM) 140 NaCl, 5.4 TEA-Cl, 2 CaCl₂, 1 MgCl₂, 10 HEPES, and 5 glucose with pH adjusted to 7.4 with NaOH. The pipette solution for I_{Ca,L} contained (in mM) 135 CsCl, 0.1 CaCl₂, 1 MgCl₂, 5 NaCl, 10 EGTA, 4 Mg-ATP, 6.6 Na-phosphocreatine, 0.3 Na-GTP and 10 HEPES, with pH adjusted to 7.2 with CsOH. To block voltage gated Na⁺ currents (I_{Na}) when recording I_{Ca,L} cells were treated with lidocaine (0.3 mM). This approach was used in order to record atrial I_{Ca,L} from a holding potential of -60 mV due to the expression of Ca_v1.2 and Ca_v1.3 in atrial myocytes.^{2,3,5,6} Thus, our voltage clamp protocols enable us to record total I_{Ca,L}, which could include contributions from Ca_v1.2 as well as Ca_v1.3.

For recording I_{Na} atrial myocytes were superfused with a modified Tyrode's solution (22 – 23°C) containing the following (in mM): 130 CsCl, 5 NaCl, 5.4 TEACl, 1 MgCl₂, 1 CaCl₂, 10 HEPES, 5.5 glucose, 5.5 (pH 7.4, adjusted with CsOH). Nitrendipine (10 µM) was added to the superfusate to block I_{Ca,L}. The pipette solution for I_{Na} contained (in mM): 120 CsCl, 5 NaCl, 1 MgCl₂, 0.2 CaCl₂, 10 HEPES, 5 MgATP, 0.3 Na-GTP, 5 BAPTA (pH 7.2, adjusted with CsOH). I_{Na} was recorded using 50 ms voltage clamp steps between -100 and 10 mV from a holding potential of -120 mV.

Micropipettes were pulled from borosilicate glass (with filament, 1.5 mm OD, 0.75 mm ID, Sutter Instrument Company) using a Flaming/Brown pipette puller (model p-87, Sutter

Instrument Company). The resistance of these pipettes was 4 – 8 M Ω when filled with recording solution. Micropipettes were positioned with a micromanipulator (Burleigh PCS-5000 system) mounted on the stage of an inverted microscope (Olympus IX71). Seal resistance was 2 – 15 G Ω . Rupturing the sarcolemma in the patch for voltage clamp experiments resulted in access resistances of 5 – 15 M Ω . Series resistance compensation averaged 80 – 85% using an Axopatch 200B amplifier (Molecular Devices). For perforated patch clamp experiments access resistance was monitored for the development of capacitive transients upon sealing to the cell membrane with Amphotericin B in the pipette. Typically, access resistance became less than 30 M Ω within 5 min of sealing onto the cell, which was sufficient for recording stimulated APs in current clamp mode. Data were digitized using a Digidata 1440 and pCLAMP 10 software (Molecular Devices) and stored on computer for analysis.

$I_{Ca,L}$ and I_{Na} activation kinetics were determined by calculating chord conductance (G) with the equation $G=I/(V_m-E_{rev})$, where V_m represents the depolarizing voltages and E_{rev} is the reversal potential estimated from the current-voltage relationships of $I_{Ca,L}$ or I_{Na} . Maximum conductance (G_{max}) and $V_{1/2}$ of activation for $I_{Ca,L}$ and I_{Na} were determined using the following function: $G=[(V_m-V_{rev})][G_{max}][1/(1+\exp((V_m-V_{1/2})/k))+1]$.

High resolution optical mapping

To study patterns of electrical conduction in the mouse atria we used high resolution optical mapping in atrial preparations as we⁷ and others^{8,9} have done previously. To isolate our atrial preparation mice were administered a 0.2 ml intraperitoneal injection of heparin (1000 IU/ml) to prevent blood clotting and were then anesthetized by isoflurane inhalation and cervically dislocated. Hearts were excised into Krebs solution (35°C) containing (in mM): 118

NaCl, 4.7 KCl, 1.2 KH₂PO₄, 12.2 MgSO₄, 1 CaCl₂, 25 NaHCO₃, 11 glucose and bubbled with 95% O₂/5% CO₂ in order to maintain a pH of 7.4. The atria were dissected away from the ventricles and pinned in a dish with the epicardial surface facing upwards (towards the imaging equipment). The superior and inferior vena cavae were cut open so that the crista terminalis could be visualized and the preparation could be pinned out flat (Supplemental Fig. 10).

The atrial preparation was superfused continuously with Krebs solution (35°C) bubbled with 95% O₂/5% CO₂ and allowed to equilibrate for at least 30 min. During this time the preparation was treated with the voltage sensitive dye di-4-ANEPPS (10 μM) for ~15 min and blebbistatin (10 μM) was added to the superfusate to suppress contractile activity.^{10,11} Blebbistatin was present throughout the duration of the experiments in order to prevent motion artifacts during optical mapping. Some experiments were performed in sinus rhythm so that the cycle length (i.e. beating rate) of the atrial preparation was free to change, while in other studies we used a pacing electrode to pace atrial preparations at a fixed cycle length in order to study electrical conduction independently of changes in cycle length. The pacing electrode was placed near the opening of the superior vena cava.

Di-4-ANEPPS loaded atrial preparations were illuminated with light at a wavelength of 520 – 570 nm using an EXFO X-cite fluorescent light source (Lumen Dynamics). Emitted light (590 – 640 nm) was captured using a high speed EMCCD camera (Evolve 128, Photometrics). Data were captured from an optical field of view of 8 x 8 mm² at a frame rate of ~1000 frames/s using Metamorph software (Molecular Devices). The spatial resolution was 67 x 67 μm for each pixel. Magnification was constant in all experiments and no pixel binning was used.

All optical data were analyzed using custom software written in Matlab. Pseudocolor electrical activation maps were generated from measurements of activation time at individual

pixels as defined by assessment of dF/dt_{\max} . In all cases background fluorescence was subtracted. Local conduction velocity (CV) was quantified specifically in the right atrial myocardium (within the RAA) and the left atrial myocardium (with in the LAA) using an established approach previously described.^{7,8,12} Briefly, activation times at each pixel from a 7 x 7 pixel array were determined and fit to a plane using the least squares fit method. The direction on this plane that is increasing the fastest represents the direction that is perpendicular to the wavefront of electrical propagation and the maximum slope represents the inverse of the speed of conduction in that direction. With a spatial resolution of 67 x 67 μM per pixel, the area of the 7 x 7 pixel array was 469 x 469 μM . Thus, using this method, we computed maximum local CV vectors in the atrial region of interest.

Optical APs (OAPs) were assessed by measuring changes in fluorescence as a function of time at individual pixels in the atrial preparation as we have previously described.^{7,13} OAPs were used to quantify changes in AP duration in the intact atrial preparation.

To measure the effects of ISO, ANP and mANP on atrial effective refractory period (ERP) we used programmed stimulation protocols in which the atrial preparation was paced at a cycle length of 90 ms for 8 beats and then given an extra stimulus at progressively shorter cycle lengths (1 ms increments).¹³ ERP was defined as the shortest coupling interval allowing for capture of the atrial preparation.

Arrhythmia studies

Susceptibility to atrial arrhythmias was studied using high resolution optical mapping in conjunction with atrial pacing. To induce arrhythmias we used S1-S2 pacing protocols in which we paced the atria at a cycle length of 90 ms (S1) and then delivered 3-6 premature extra beats at

shorter cycle lengths (50 or 25 ms). In all arrhythmia studies the atrial preparations were in normal sinus rhythm and displayed normal patterns of electrical activation and conduction before atrial pacing took place.

Quantitative PCR

A portion of our human right atrial samples was retained for molecular biology studies. Quantitative gene expression in human right atrial tissue was performed using methods similar to those we have previously described in mice.^{2,3} Intron spanning primers were designed for human Npr1, Npr2 and Npr3 (genes corresponding to NPR-A, NPR-B and NPR-C) as well as GAPDH, which was used as a reference gene. Following synthesis (Sigma Genosys) primers were reconstituted in nuclease free water at a concentration of 100 nM and frozen at -20°C. Primer sequences were as follows:

Npr1:

Forward 5'-TCACGCACGCTACAAACA-3'

Reverse 5'-GAGAGAGAGAGAGAGAGAGAAAGG-3'

Amplification product: 106 base pairs

Npr2:

Forward 5'-GACGACCCATCCTGTGATAAA-3'

Reverse 5'-GGAAGCTGGAAACACCAAAC-3'

Amplification product: 97 base pairs

Npr3:

Forward 5'-GTGGGTTAGGTGTGGAGATAAG-3'

Reverse 5'-CTACTGGGTGCAAAGCAGATA-3'

Amplification product: 77 base pairs

GAPDH:

Forward 5'-ATGACATCAAGAAGGTGGTG-3'

Reverse 5'-CATACCAGGAAATGAGCTTG-3'

Amplification product: 177 base pairs

RNA was extracted in PureZOL™ RNA isolation reagent according to kit instructions (Aurum total RNA fatty and fibrous tissue kit, BioRad). Tissue was eluted in 30-40 µl of elution buffer from the spin column. RNA concentrations were determined using a Qubit fluorometer (Invitrogen) and first strand synthesis reactions were performed using the iScript cDNA synthesis kit (BioRad) according to kit instructions with 0.5 µg RNA template. A260/280 readings were also performed to evaluate the purity of RNA extractions prior to first strand synthesis. Lack of genomic DNA contamination was verified by reverse transcription (RT)-PCR using a no RT control.

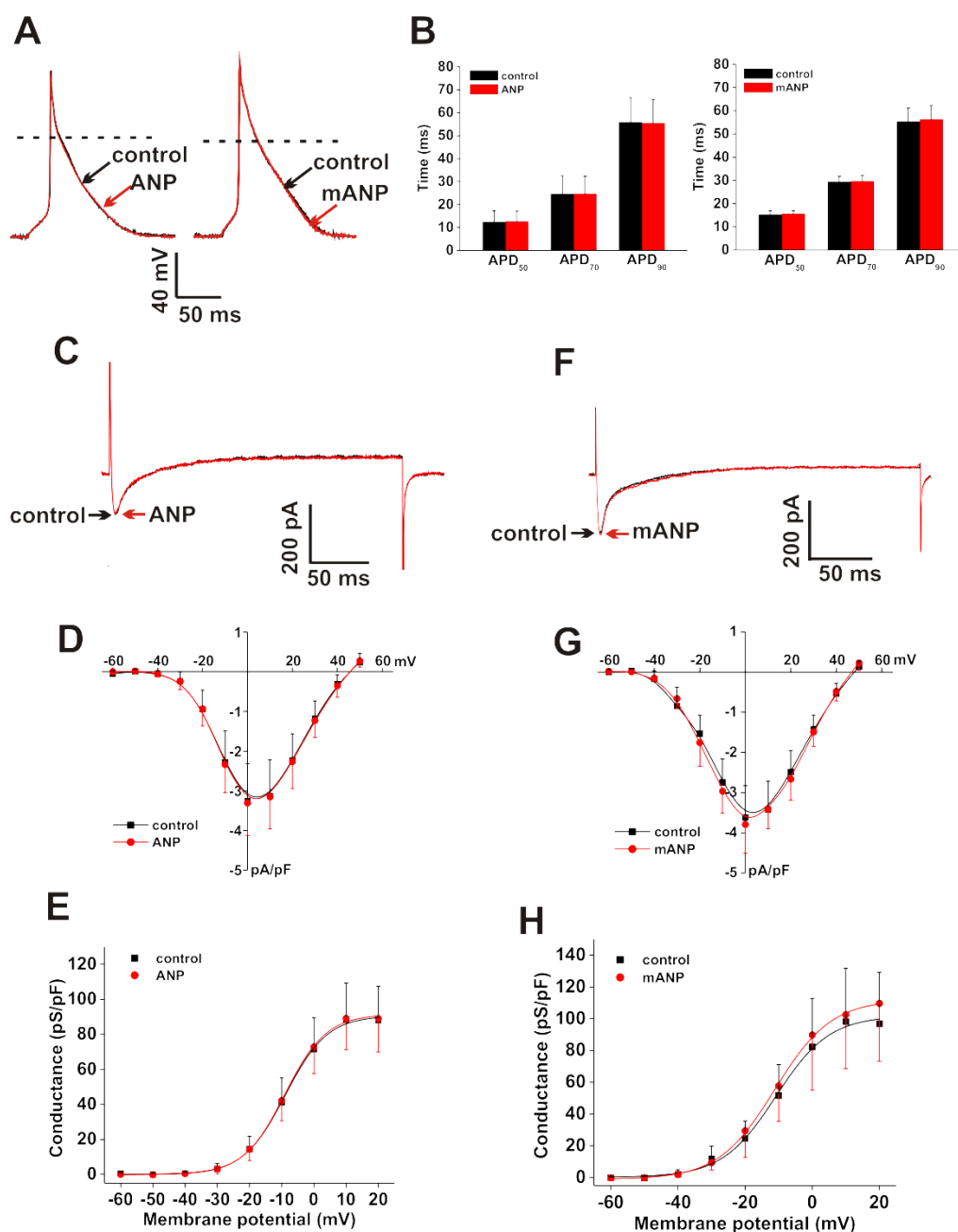
RT-qPCR using BRYT green dye was used to assess gene expression. Following RNA extraction cDNA was synthesized and 20 µl BRYT reactions were performed with 1 µl cDNA template. Reactions were carried out using a CFX96 Real-Time PCR Detection System (BioRad). Amplification conditions were as follows: 95°C for 2 min to activate Taq polymerase, 35 cycles of denaturation at 95°C for 30 sec, annealing using a gradient from 53-61°C for 30 sec and extension at 72°C or 1 min 30 sec. Melt curve analysis was performed from 65-95°C every 0.5°C increments. Single amplicons with appropriate melting temperatures and sizes were

detected. Data were expressed in the form $2^{-\Delta CT} \times 100$ vs. GAPDH for all tissue samples. C_T values > 32 were eliminated due to lack of reproducibility.¹⁴ Primers were used at a concentration of 10 nM.

cAMP assay

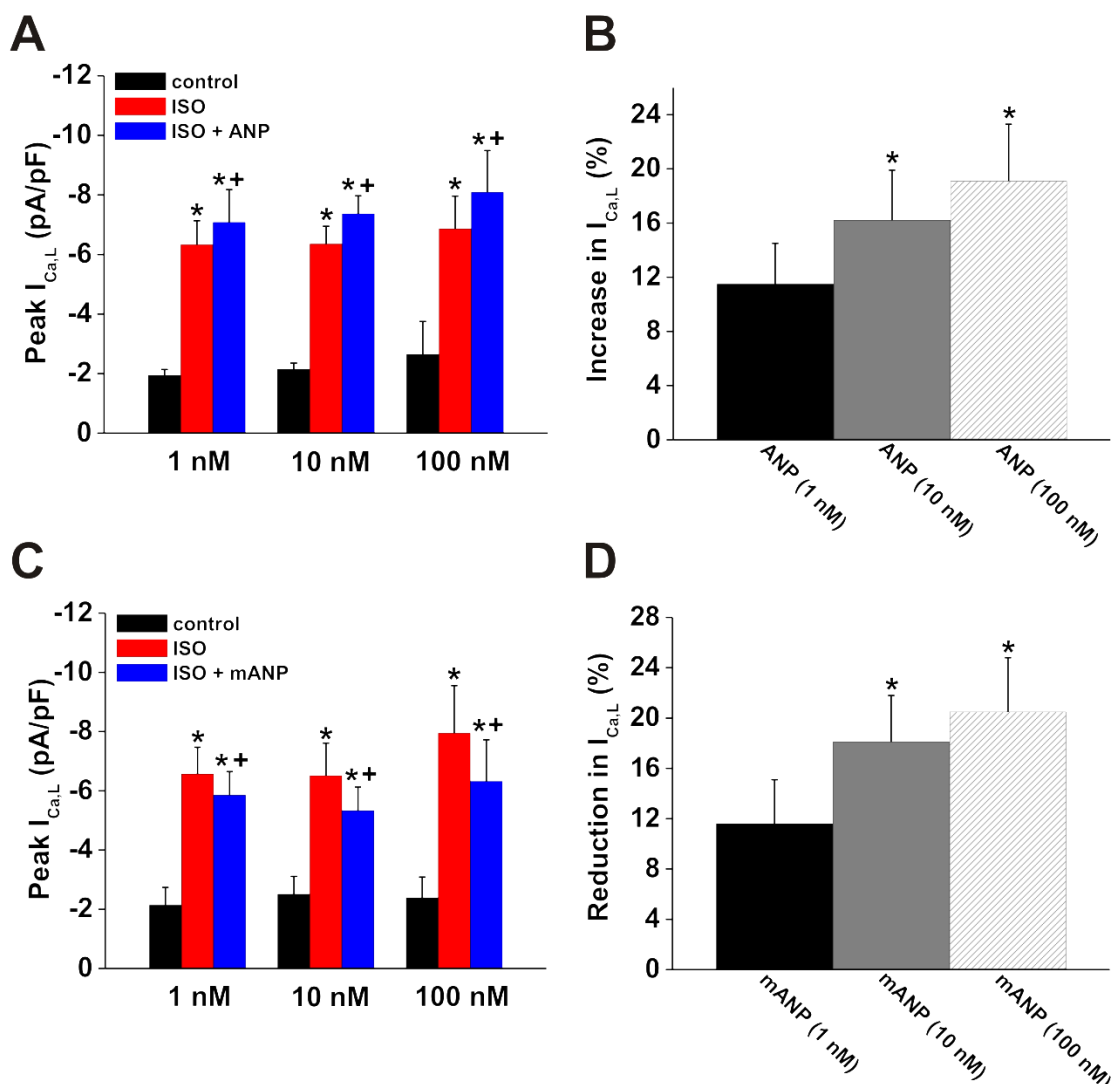
Mouse right atrial myocytes were isolated as described above and centrifuged (2000 rpm) for 5 minutes. The supernatant was removed and the pellet was resuspended in normal Tyrode's solution. A hemocytometer was used to determine myocyte density. Cells were either untreated (control) or treated with the following: ANP alone, mANP alone, ISO, ISO + ANP or ISO + mANP. Cells were incubated with these compounds for 15 min at 4°C. Intracellular cAMP concentrations were then determined using a HTRF cAMP Femto2 kit (Cisbio US) according to the manufacturer's instructions.

Results

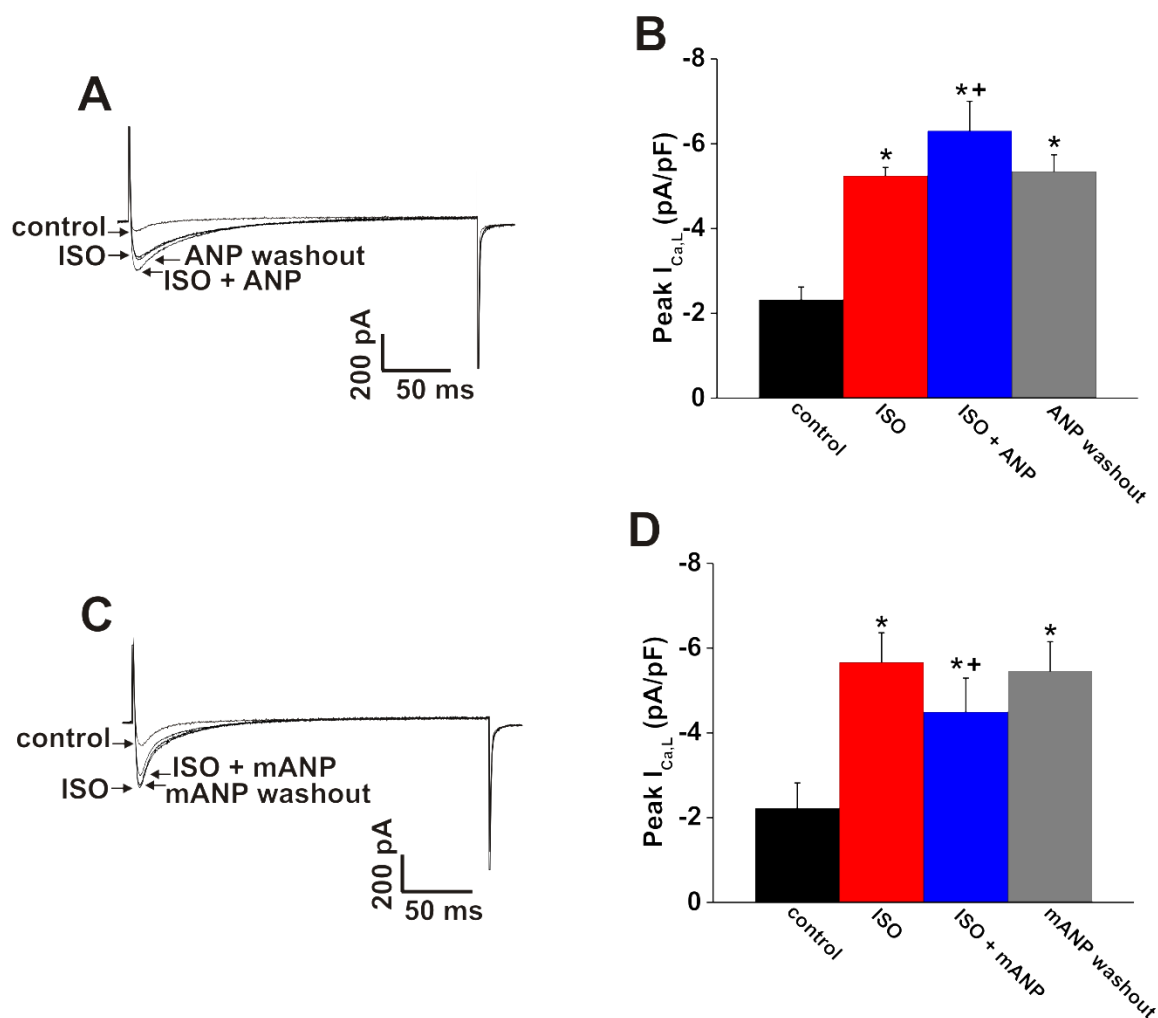


Supplemental Figure 1: Effects of ANP and mANP on mouse atrial action potential morphology and L-type Ca^{2+} current in basal conditions. **A**, Representative right atrial APs in control conditions and after application of ANP (100 nM) or mANP (100 nM). **B**, Summary of the effects of ANP and mANP on right atrial AP duration at 50% (APD_{50}), 70% (APD_{70}) and 90% (APD_{90}) repolarization. ANP and mANP had no effect on atrial AP duration. Data analyzed by paired Student's *t*-test; $n=6$ myocytes for ANP and 5 myocytes for mANP. Refer to Supplemental Tables 2 and 3 for additional AP parameters. **C**, Representative right atrial $\text{I}_{\text{Ca,L}}$ recordings in control conditions and after application of ANP (100 nM). **D**, Right atrial $\text{I}_{\text{Ca,L}}$ IV relationships in control conditions and after application of ANP. **E**, Summary $\text{I}_{\text{Ca,L}}$ conductance density plots demonstrating the effects of ANP on $\text{I}_{\text{Ca,L}}$ activation kinetics. **F**,

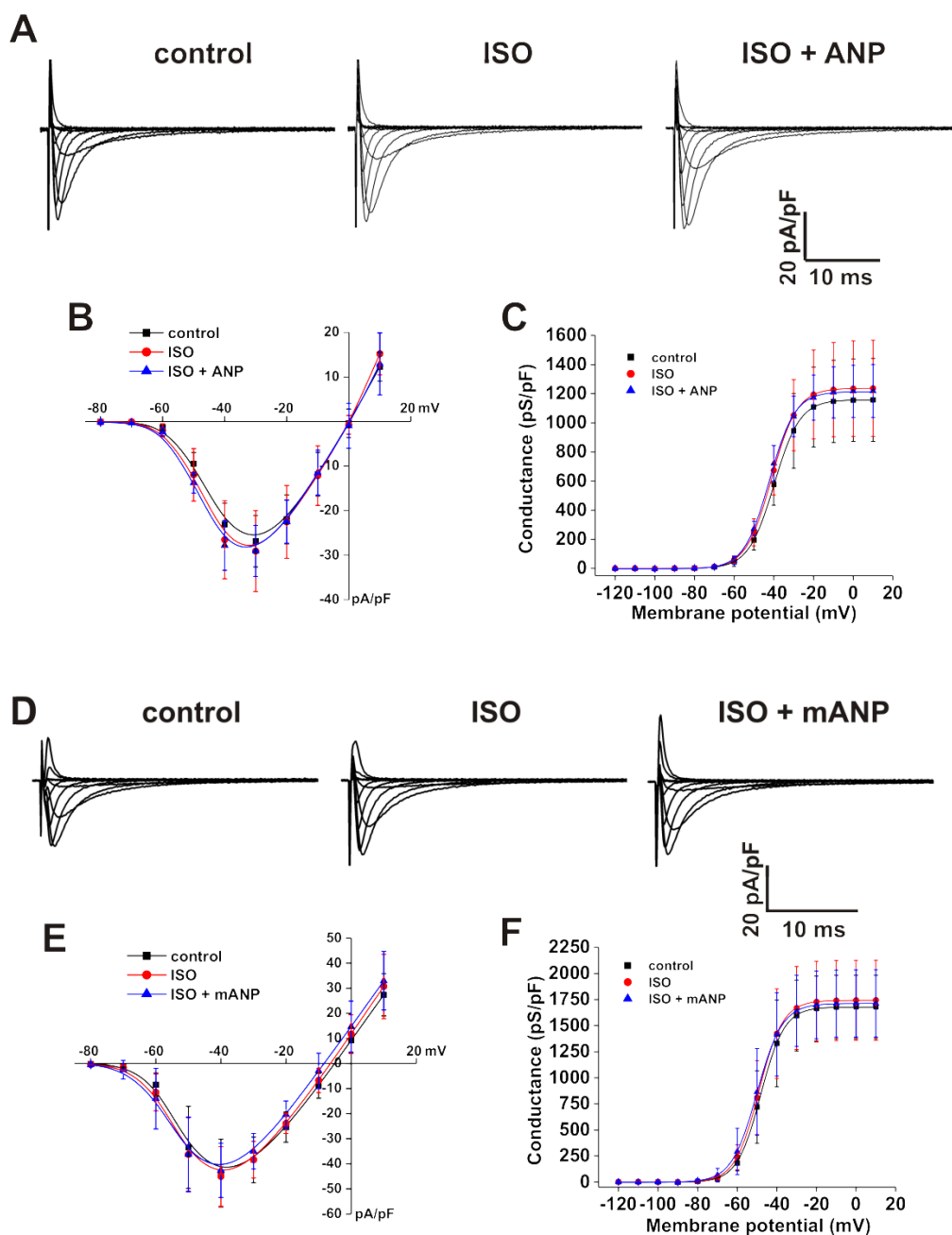
Representative right atrial $I_{Ca,L}$ recordings in control conditions and after application of mANP (100 nM). **G**, Right atrial $I_{Ca,L}$ IV relationships in control conditions and after application of mANP. **H**, Summary $I_{Ca,L}$ conductance density plots demonstrating the effects of mANP on $I_{Ca,L}$ activation kinetics. Neither ANP ($n=7$ myocytes) or mANP ($n=5$ myocytes) had any effects on mouse right atrial $I_{Ca,L}$. Refer to Supplemental Tables 4 and 5 for analysis of $I_{Ca,L}$ activation kinetics.



Supplemental Figure 2: Dose dependence of the effects of ANP and mANP on mouse atrial $I_{Ca,L}$ in the presence of isoproterenol. (A) Summary of the effects of ISO (10 nM) and ANP (1, 10, 100 nM) on peak $I_{Ca,L}$ (measured at 0 mV) in mouse right atrial myocytes. * $P < 0.05$ vs. control; + $P < 0.05$ vs. ISO by one-way repeated measures ANOVA with Tukey's posthoc test; $n = 5$ myocytes for 1 nM dose, 5 myocytes for 10 nM dose and 8 myocytes for 100 nM dose of ANP. (B) Summary data demonstrating the percent increase in $I_{Ca,L}$ (in the presence of ISO) elicited by each dose of ANP. * $P < 0.05$ vs. 1 nM dose by one-way ANOVA with Tukey's posthoc test. (C) Summary of the effects of ISO (10 nM) and mANP (1, 10, 100 nM) on peak $I_{Ca,L}$ (measured at 0 mV) in mouse right atrial myocytes. * $P < 0.05$ vs. control; + $P < 0.05$ vs. ISO by one-way repeated measures ANOVA with Tukey's posthoc test; $n = 5$ myocytes for 1 nM dose, 5 myocytes for 10 nM dose and 6 myocytes for 100 nM dose of ANP. (D) Summary data demonstrating the percent decrease in $I_{Ca,L}$ (in the presence of ISO) elicited by each dose of mANP. * $P < 0.05$ vs. 1 nM dose by one-way ANOVA with Tukey's posthoc test.

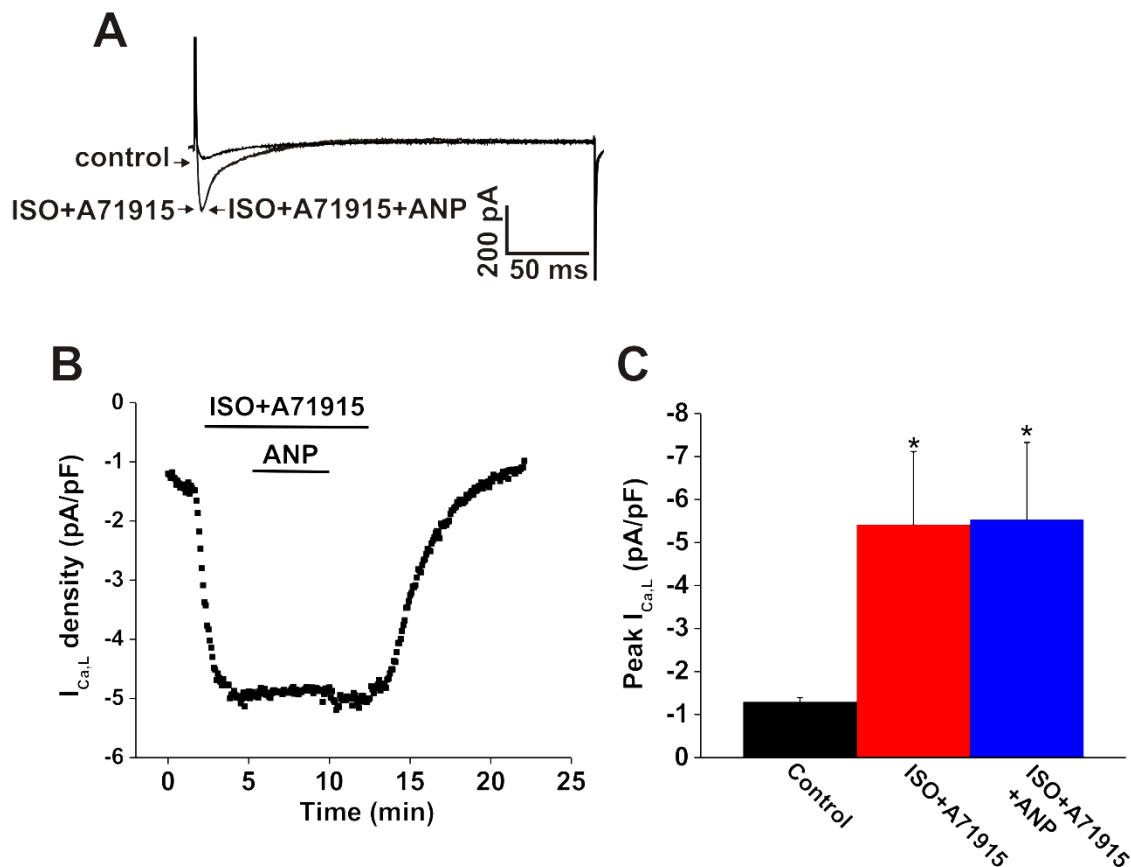


Supplemental Figure 3: Effects of ANP and mANP on $I_{Ca,L}$ in mouse left atrial myocytes. (A) Representative left atrial $I_{Ca,L}$ recordings in control conditions, in the presence of ISO (10 nM), after application of ANP (100 nM) in the presence of ISO, and after ANP washout. (B) Summary of the effects of ISO and ANP on left atrial $I_{Ca,L}$ in mice. * $P < 0.05$ vs. control; + $P < 0.05$ vs. ISO by one-way repeated measures ANOVA with Tukey's posthoc test; $n = 6$ myocytes. (C) Representative left atrial $I_{Ca,L}$ recordings in control conditions, in the presence of ISO (10 nM), after application of mANP (100 nM) in the presence of ISO, and following mANP washout. (D) Summary of the effects of ISO and mANP on left atrial $I_{Ca,L}$ in mice. * $P < 0.05$ vs. control; $P < 0.05$ vs. ISO by one-way repeated measures ANOVA with Tukey's posthoc test; $n = 6$ myocytes.

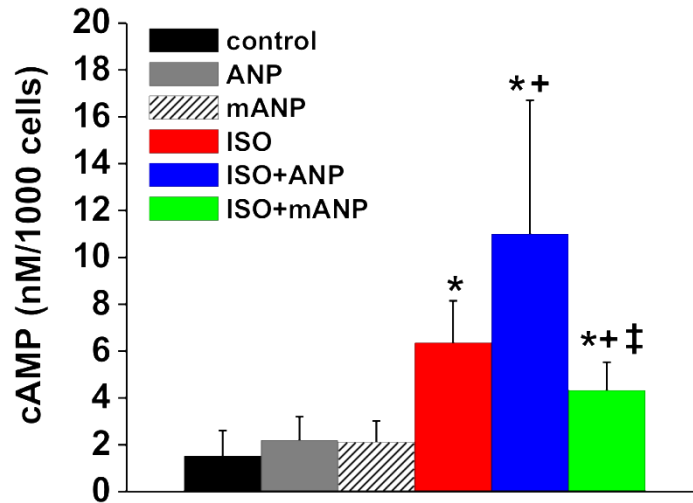


Supplemental Figure 4: Effects of ANP and mANP on mouse atrial I_{Na} in the presence of isoproterenol. (A) Representative right atrial I_{Na} recordings in control conditions, in the presence of ISO (10 nM) and after application of ANP (100 nM) in the presence of ISO. (B) Right atrial I_{Na} IV relationships in control conditions, in the presence of ISO and after the application of ANP in the presence of ISO. There was no significant effect of ISO or ANP in I_{Na} density ($P=0.511$ by one-way repeated measures ANOVA); $n=5$ myocytes. (C) Summary I_{Na} conductance density plots demonstrating the effects of ISO and ANP on I_{Na} activation kinetics. Refer to Supplemental Table 13 for analysis of I_{Na} activation kinetics. (D) Representative right atrial I_{Na} recordings in control conditions, in the presence of ISO (10 nM) and after application of

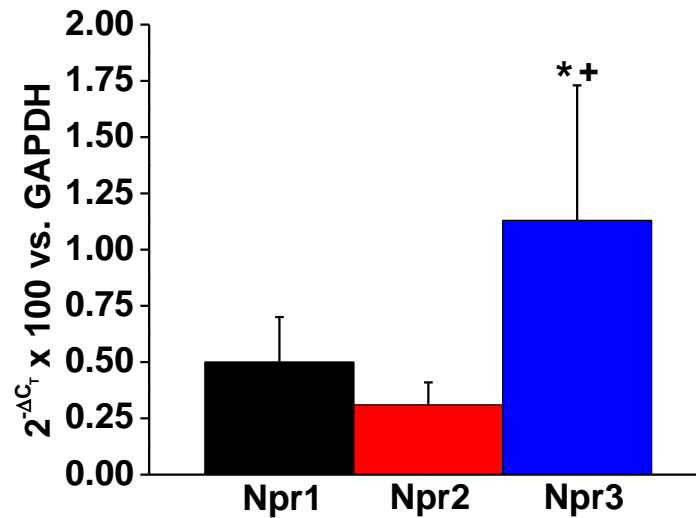
mANP (100 nM) in the presence of ISO. **(E)** Right atrial I_{Na} IV relationships in control conditions, in the presence of ISO and after the application of mANP in the presence of ISO. There was no significant effect of ISO or mANP in I_{Na} density ($P=0.717$ by one-way repeated measures ANOVA); $n=6$ myocytes. **(F)** Summary I_{Na} conductance density plots demonstrating the effects of ISO and mANP on I_{Na} activation kinetics. Refer to Supplemental Table 14 for analysis of I_{Na} activation kinetics.



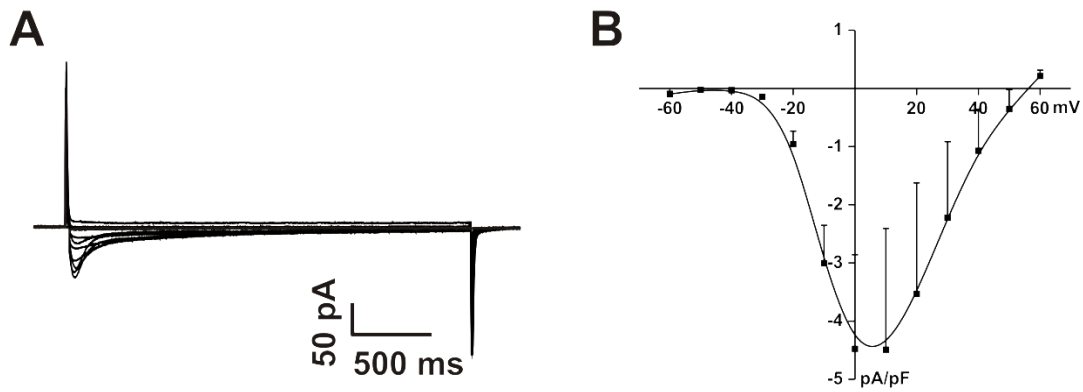
Supplemental Figure 5: The effects of ANP on atrial $I_{Ca,L}$ are blocked by the NPR-A antagonist A71915. (A) Representative $I_{Ca,L}$ recordings (at 0 mV) in control conditions, in the presence of ISO (10 nM) and A71915 (500 nM) and following application of ANP (100 nM) in the presence of ISO and A71915. (B) Time course of the effects of ISO, A71915 and ANP on $I_{Ca,L}$. (C) Summary of the effects of ISO, A71915 and ANP on peak $I_{Ca,L}$ in right atrial myocytes. * $P < 0.05$ vs. control by one-way repeated measures ANOVA with Tukey's posthoc test; ANP had no effect ($P = 0.991$) on $I_{Ca,L}$ amplitude following NPR-A blockade; $n = 5$ myocytes.



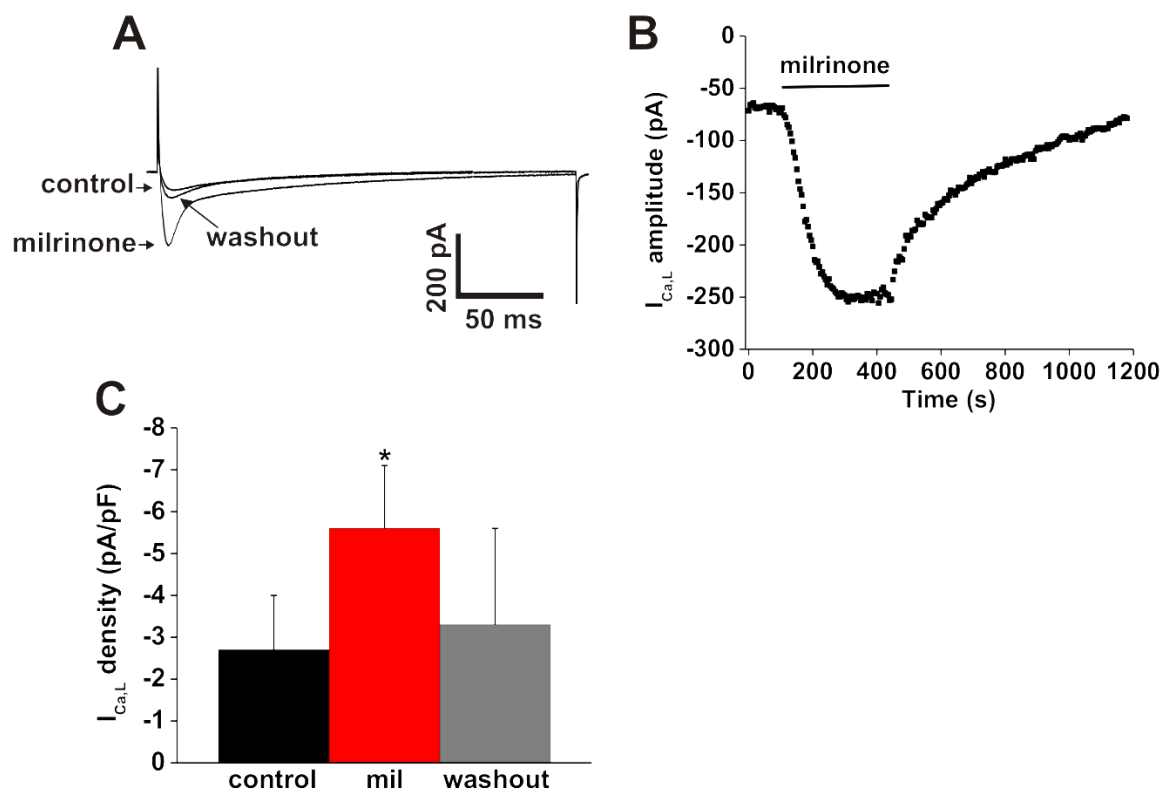
Supplemental Figure 6: ANP and mANP have opposing effects on intracellular cAMP production in right atrial myocytes. The effects of ANP (100 nM) and mANP (100 nM) on cAMP production were measured in basal conditions and after application of ISO (10 nM). * $P < 0.05$ vs. control; † $P < 0.05$ vs. ISO; ‡ $P < 0.05$ vs. ISO+ANP by one-way ANOVA with Tukey's posthoc test; $n = 6$ right atrial myocyte isolations.



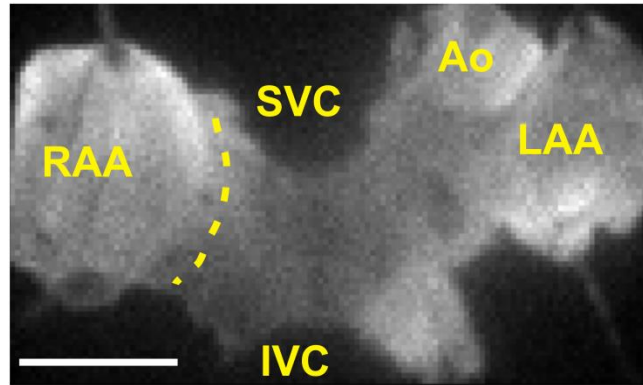
Supplemental Figure 7: Quantitative mRNA expression of natriuretic peptide receptors in human right atrial myocardium. Expression is shown for Npr1, Npr2 and Npr3, which correspond to NPR-A, NPR-B and NPR-C respectively, relative to GAPDH. * $P < 0.05$ vs. Npr1, ⁺ $P < 0.05$ vs. Npr2 by one-way ANOVA with Tukey's posthoc test; $n = 10$ human right atrial samples.



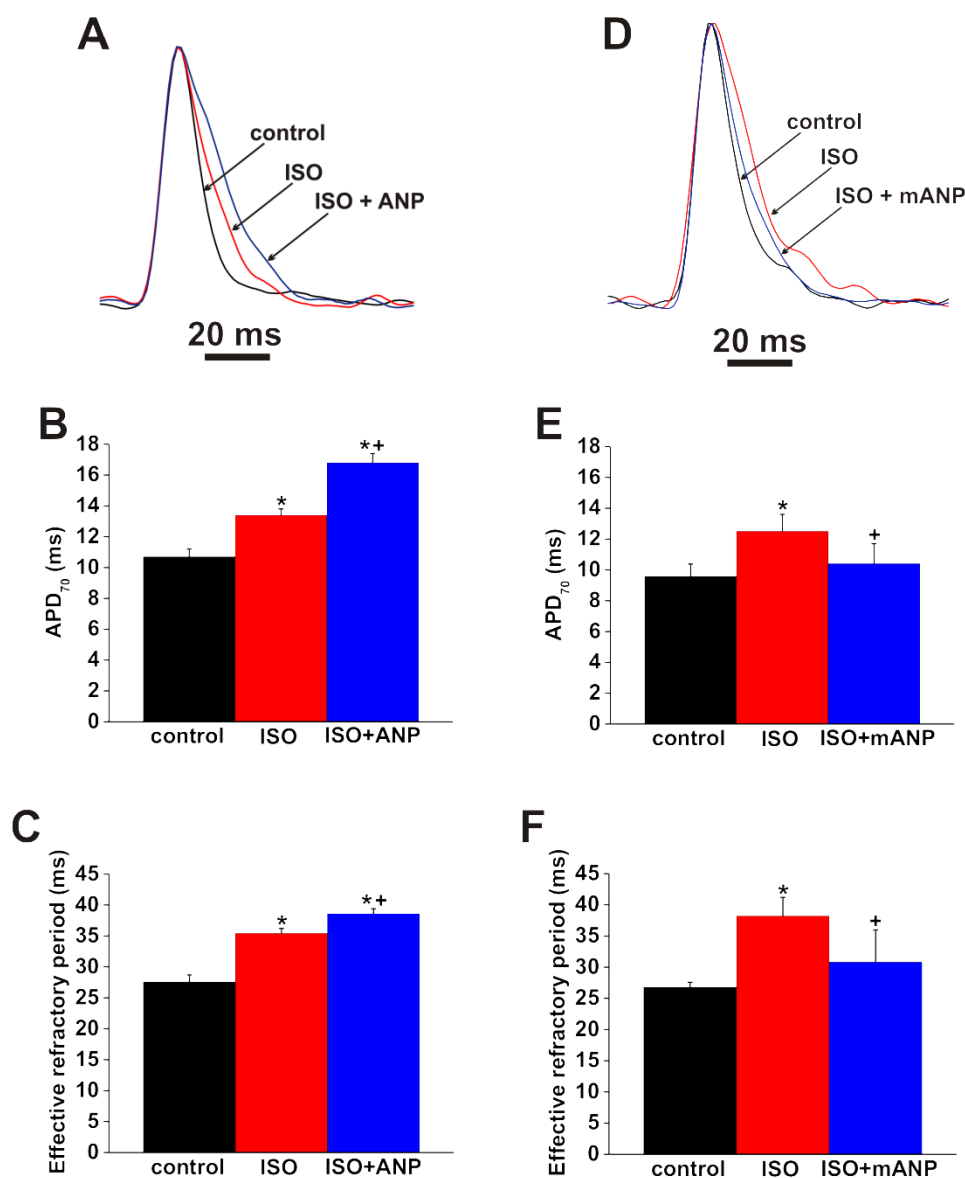
Supplemental Figure 8: Properties of L-type Ca^{2+} current in human right atrial myocytes. (A) Representative example of a family of $I_{\text{Ca,L}}$ recordings between -60 mV and +60 mV (holding potential = -60 mV). (B) Human $I_{\text{Ca,L}}$ IV relationship; $n=5$ right atrial myocytes from 3 patient samples.



Supplemental Figure 9: Effects of the PDE3 inhibitor milrinone on basal $I_{Ca,L}$ in human right atrial myocytes. (A) Representative $I_{Ca,L}$ recordings (at 0 mV) in basal conditions, after application of milrinone (10 μ M) and after washout of milrinone. (B) Time course of the effects of milrinone on human atrial $I_{Ca,L}$. (C) Summary of the effects of milrinone on human atrial $I_{Ca,L}$. * $P < 0.05$ vs. control by one-way repeated measures ANOVA with Tukey's posthoc test; $n = 7$ myocytes from 4 patient samples.



Supplemental Figure 10: Atrial preparation used for high resolution optical mapping studies. The preparation is oriented with the right atrium on the left side of the image. RAA, right atrial appendage; SVC, opening of superior vena cava; IVC, opening of inferior vena cava; LAA, left atrial appendage; Ao, aorta. The crista terminalis is shown by the dashed line. Scale bar is 2 mm.



Supplemental Figure 11: Effects of ANP and mANP on action potential duration and effective refractory period in mouse atrial preparations. **(A)** Representative optical APs (OAPs) in control conditions, in the presence of ISO (10 nM) and after application of ANP (50 nM) in the presence of ISO. OAPs were measured in the right atrial appendage using high resolution optical mapping. **(B)** Summary of the effects of ISO and ANP on APD₇₀ in mouse right atrium. **(C)** Summary of the effects of ISO and ANP on atrial effective refractory period. For panels B and C * $P < 0.05$ vs. control; ⁺ $P < 0.05$ vs. ISO by one-way repeated measures ANOVA; $n = 5$ hearts. **(D)** Representative optical APs (OAPs) in control conditions, in the presence of ISO (10 nM) and after application of mANP (50 nM) in the presence of ISO. **(E)** Summary of the effects of ISO and mANP on APD₇₀ in mouse right atrium. **(F)** Summary of the effects of ISO and mANP on atrial effective refractory period. For panels E and F * $P < 0.05$ vs. control; ⁺ $P < 0.05$ vs. ISO by one-way repeated measures ANOVA; $n = 5$ hearts.

Supplemental Table 1: Patient characteristics

Patients (<i>n</i>)	15
Gender (M/F)	13/2
Age (years)	61.4±10.9
Weight (kg)	90.4±17.9
BMI (kg/m ²)	30.2±3.9
CAD (<i>n</i>)	14
Dyslipidemia (<i>n</i>)	11
Diabetes (<i>n</i>)	6
Valve disease (<i>n</i>)	1
Hypertension (<i>n</i>)	8
β-blockers (<i>n</i>)	10
ACE inhibitors/ARB (<i>n</i>)	10
Ca ²⁺ channel blockers (<i>n</i>)	4
Nitrates (<i>n</i>)	10
Diuretics (<i>n</i>)	2
Lipid lowering drugs (<i>n</i>)	14

BMI, body mass index; CAD, coronary artery disease; ACE, angiotensin converting enzyme; ARB, angiotensin receptor blocker.

Supplemental Table 2: Action potential parameters at baseline and after application of ANP (100 nM) in mouse right atrial myocytes

	Control	ANP
RMP (mV)	-77.9 ± 0.7	-78.0 ± 0.7
V _{max} (V/s)	150.0 ± 17.0	149.3 ± 16.8
OS (mV)	60.3 ± 15.8	60.1 ± 16.3
APD ₅₀ (ms)	12.4 ± 4.8	12.6 ± 4.6
APD ₇₀ (ms)	24.6 ± 7.9	24.7 ± 7.7
APD ₉₀ (ms)	55.8 ± 10.8	55.5 ± 10.3

RMP, resting membrane potential; V_{max}, AP upstroke velocity; OS, overshoot; APD₅₀, AP duration at 50% repolarization; APD₇₀, AP duration at 70% repolarization; APD₉₀, AP duration at 90% repolarization. ANP had no effects on these AP parameters. Data analyzed by paired Student's *t*-test; *n*=6 myocytes.

Supplemental Table 3: Action potential parameters at baseline and after application of mANP (100 nM) in mouse right atrial myocytes

	Control	mANP
RMP (mV)	-77.4 ± 0.9	-77.8 ± 0.7
V_{\max} (V/s)	144.2 ± 11.7	143.8 ± 11.0
OS (mV)	60.8 ± 8.6	59.8 ± 7.7
APD ₅₀ (ms)	15.2 ± 1.8	15.6 ± 1.3
APD ₇₀ (ms)	29.3 ± 2.4	29.6 ± 2.6
APD ₉₀ (ms)	55.3 ± 5.9	56.3 ± 5.9

RMP, resting membrane potential; V_{\max} , AP upstroke velocity; OS, overshoot; APD₅₀, AP duration at 50% repolarization; APD₇₀, AP duration at 70% repolarization; APD₉₀, AP duration at 90% repolarization. ANP had no effects on these AP parameters. Data analyzed by paired Student's *t*-test; *n*=5 myocytes.

Supplemental Table 4: $I_{Ca,L}$ conductance analysis in baseline conditions and following application of ANP in mouse right atrial myocytes

	Control	ANP
G_{\max} (pS/pF)	90.7 ± 3.4	91.6 ± 3.1
$V_{1/2(\text{act})}$ (mV)	-8.9 ± 1.0	-9.1 ± 1.0
k	6.5 ± 1.0	6.4 ± 0.8

G_{\max} , maximum conductance; $V_{1/2(\text{act})}$, voltage at which 50% of channels are activated; k, slope factor. ANP had no effects on $I_{Ca,L}$ activation kinetics. Data analyzed by Student's *t*-test; *n*=7 myocytes.

Supplemental Table 5: $I_{Ca,L}$ conductance analysis in baseline conditions and following application of mANP in mouse right atrial myocytes

	Control	mANP
G_{\max} (pS/pF)	101.8 ± 6.4	112.0 ± 3.3
$V_{1/2(\text{act})}$ (mV)	-10.9 ± 2.0	-11.1 ± 0.9
k	7.9 ± 1.8	8.4 ± 0.9

G_{\max} , maximum conductance; $V_{1/2(\text{act})}$, voltage at which 50% of channels are activated; k, slope factor. ANP had no effects on $I_{Ca,L}$ activation kinetics. Data analyzed by Student's *t*-test; *n*=5 myocytes.

Supplemental Table 6: Action potential parameters at baseline and after application of ISO (10 nM) and ANP (10 nM) in mouse right atrial myocytes

	Control	ISO	ISO + ANP	ANP washout
RMP (mV)	-80.9 ± 2.4	-80.3 ± 2.0	-80.8 ± 2.4	-80.4 ± 2.0
V _{max} (V/s)	139.5 ± 17.6	145.7 ± 18.0*	151.5 ± 18.5* ⁺	144.5 ± 20.7*
OS (mv)	57.3 ± 5.1	62.6 ± 2.6	64.2 ± 2.9*	63.2 ± 3.1
APD ₅₀ (ms)	10.0 ± 4.4	16.5 ± 7.9*	20.7 ± 8.6*	17.5 ± 7.0*
APD ₇₀ (ms)	19.7 ± 3.1	32.7 ± 5.7*	42.5 ± 7.0* ⁺	33.4 ± 7.0*
APD ₉₀ (ms)	46.1 ± 4.8	63.6 ± 3.7*	76.8 ± 7.3* ⁺	65.5 ± 3.5*

RMP, resting membrane potential; V_{max}, AP upstroke velocity; OS, overshoot; APD₅₀, AP duration at 50% repolarization; APD₇₀, AP duration at 70% repolarization; APD₉₀, AP duration at 90% repolarization. **P*<0.05 vs control, ⁺*P*<0.05 vs. ISO by one-way repeated measures ANOVA with Tukey's posthoc test; *n*=5 myocytes.

Supplemental Table 7: Action potential parameters at baseline and after application of ISO (10 nM) and ANP (100 nM) in mouse right atrial myocytes

	Control	ISO	ISO + ANP	ANP washout
RMP (mV)	-82.4 ± 0.9	-82.5 ± 1.7	-82.3 ± 1.9	-82.1 ± 1.9
V _{max} (V/s)	157.4 ± 12.7	173.9 ± 12.5*	183.2 ± 9.4* ⁺	173.6 ± 11.8*
OS (mv)	59.6 ± 3.8	64.9 ± 4.6*	68.0 ± 4.6*	64.8 ± 5.0*
APD ₅₀ (ms)	11.8 ± 4.6	15.5 ± 5.5*	19.5 ± 7.0* ⁺	15.6 ± 5.8*
APD ₇₀ (ms)	20.3 ± 8.2	27.6 ± 10.8*	36.7 ± 13.4* ⁺	27.9 ± 11.0*
APD ₉₀ (ms)	46.5 ± 10.8	58.3 ± 10.3*	71.5 ± 11.8* ⁺	58.7 ± 11.0*

RMP, resting membrane potential; V_{max}, AP upstroke velocity; OS, overshoot; APD₅₀, AP duration at 50% repolarization; APD₇₀, AP duration at 70% repolarization; APD₉₀, AP duration at 90% repolarization. **P*<0.05 vs control, ⁺*P*<0.05 vs. ISO by one-way repeated measures ANOVA with Tukey's posthoc test; *n*=6 myocytes.

Supplemental Table 8: Action potential parameters at baseline and after application of ISO (10 nM) and mANP (10 nM) in mouse right atrial myocytes

	Control	ISO	ISO + mANP	mANP washout
RMP (mV)	-80.0 ± 1.0	-80.2 ± 1.3	-80.3 ± 1.3	-80.4 ± 1.3
V _{max} (V/s)	130.4 ± 8.8	152.1 ± 11.7*	144.7 ± 9.6* ⁺	151.8 ± 12.5*
OS (mv)	56.5 ± 5.2	63.1 ± 6.0*	57.8 ± 7.3	62.7 ± 6.5*
APD ₅₀ (ms)	7.8 ± 3.4	13.6 ± 4.4*	11.4 ± 3.9*	13.7 ± 4.4*
APD ₇₀ (ms)	18.7 ± 5.5	28.7 ± 7.0*	23.5 ± 6.5* ⁺	27.5 ± 7.5*
APD ₉₀ (ms)	45.5 ± 5.7	58.0 ± 8.3*	51.4 ± 7.5* ⁺	56.2 ± 9.4*

RMP, resting membrane potential; V_{max}, AP upstroke velocity; OS, overshoot; APD₅₀, AP duration at 50% repolarization; APD₇₀, AP duration at 70% repolarization; APD₉₀, AP duration at 90% repolarization. **P*<0.05 vs control, ⁺*P*<0.05 vs. ISO by one-way repeated measures ANOVA with Tukey's posthoc test; *n*=7 myocytes.

Supplemental Table 9: Action potential parameters at baseline and after application of ISO (10 nM) and mANP (100 nM) in mouse right atrial myocytes

	Control	ISO	ISO + mANP	mANP washout
RMP (mV)	-81.3 ± 1.5	-81.7 ± 1.5	-81.6 ± 0.9	-81.0 ± 2.1
V _{max} (V/s)	146.4 ± 15.0	169.4 ± 15.6*	157.9 ± 19.5* ⁺	165.2 ± 16.5*
OS (mv)	63.0 ± 5.4	67.6 ± 5.1*	63.3 ± 4.5	65.6 ± 5.1
APD ₅₀ (ms)	10.9 ± 3.3	15.0 ± 3.0*	12.1 ± 3.6* ⁺	15.9 ± 5.7*
APD ₇₀ (ms)	22.0 ± 2.1	30.9 ± 4.5*	24.0 ± 3.9 ⁺	29.4 ± 6.9*
APD ₉₀ (ms)	47.9 ± 6.0	60.8 ± 6.3*	54.1 ± 5.7* ⁺	59.1 ± 7.5*

RMP, resting membrane potential; V_{max}, AP upstroke velocity; OS, overshoot; APD₅₀, AP duration at 50% repolarization; APD₇₀, AP duration at 70% repolarization; APD₉₀, AP duration at 90% repolarization. **P*<0.05 vs control, ⁺*P*<0.05 vs. ISO by one-way repeated measures ANOVA with Tukey's posthoc test; *n*=9 myocytes.

Supplemental Table 10: Action potential parameters at baseline and after application of ISO (10 nM) and ANP + mANP (100 nM each) in mouse right atrial myocytes

	Control	ISO	ISO + ANP + mANP	ANP/mANP washout
RMP (mV)	-80.0 ± 2.3	-79.8 ± 1.8	-80.8 ± 2.1	-80.1 ± 1.8
V _{max} (V/s)	133.9 ± 22.6	146.0 ± 21.6*	142.0 ± 23.4*	143.1 ± 25.2*
OS (mv)	59.5 ± 7.3	64.6 ± 7.8*	61.2 ± 9.6	62.4 ± 9.1
APD ₅₀ (ms)	7.0 ± 3.1	12.1 ± 4.2*	11.3 ± 3.9*	12.1 ± 4.4*
APD ₇₀ (ms)	18.4 ± 9.6	28.3 ± 12.2*	25.9 ± 12.0*	27.2 ± 11.4*
APD ₉₀ (ms)	49.6 ± 15.3	62.2 ± 15.9*	58.1 ± 14.6*	61.2 ± 13.3*

RMP, resting membrane potential; V_{max}, AP upstroke velocity; OS, overshoot; APD₅₀, AP duration at 50% repolarization; APD₇₀, AP duration at 70% repolarization; APD₉₀, AP duration at 90% repolarization. **P*<0.05 vs control, by one-way repeated measures ANOVA with Tukey's posthoc test; *n*=7 myocytes.

Supplemental Table 11: I_{Ca,L} conductance analysis in baseline conditions and following application of ISO and ANP in mouse right atrial myocytes

	Control	ISO	ISO + ANP
G _{max} (pS/pF)	79.3 ± 0.8	168.1 ± 6.4*	194.7 ± 6.7* ⁺
V _{1/2(act)} (mV)	-10.2 ± 0.3	-16.3 ± 1.1*	-18.6 ± 1.1* ⁺
k	7.4 ± 0.3	6.6 ± 0.8	6.5 ± 0.8

G_{max}, maximum conductance; V_{1/2(act)}, voltage at which 50% of channels are activated; k, slope factor. **P*<0.05 vs control, ⁺*P*<0.05 vs. ISO by one-way repeated measures ANOVA with Tukey's posthoc test; *n*=8 myocytes.

Supplemental Table 12: $I_{Ca,L}$ conductance analysis in baseline conditions and following application of ISO and mANP in mouse right atrial myocytes

	Control	ISO	ISO + mANP
G_{max} (pS/pF)	72.5 ± 3.1	$178.2 \pm 7.9^*$	$152.9 \pm 5.3^{*+}$
$V_{1/2(act)}$ (mV)	-12.0 ± 0.5	$-20.6 \pm 1.4^*$	$-18.5 \pm 1.0^{*+}$
k	7.8 ± 1.0	5.7 ± 1.2	6.3 ± 1.0

G_{max} , maximum conductance; $V_{1/2(act)}$, voltage at which 50% of channels are activated; k, slope factor. * $P < 0.05$ vs control, + $P < 0.05$ vs. ISO by one-way repeated measures ANOVA with Tukey's posthoc test; $n=6$ myocytes.

Supplemental Table 13: I_{Na} conductance analysis in baseline conditions and following application of ISO and ANP in mouse right atrial myocytes

	Control	ISO	ISO + ANP
G_{max} (pS/pF)	1167.3 ± 8.6	1240.7 ± 5.7	1219.3 ± 11.2
$V_{1/2(act)}$ (mV)	-39.7 ± 0.2	-41.3 ± 0.2	-42.0 ± 0.4
k	6.7 ± 0.2	6.5 ± 0.2	6.6 ± 0.2

G_{max} , maximum conductance; $V_{1/2(act)}$, voltage at which 50% of channels are activated; k, slope factor. There were no significant effects of ISO or ANP on I_{Na} G_{max} ($P=0.658$), $V_{1/2(act)}$ ($P=0.235$) or k ($P=0.67$). Data analyzed by one-way repeated measures ANOVA; $n=5$ myocytes.

Supplemental Table 14: I_{Na} conductance analysis in baseline conditions and following application of ISO and mANP in mouse right atrial myocytes

	Control	ISO	ISO + mANP
G_{max} (pS/pF)	1679.2 ± 21.1	1752.8 ± 13.0	1709.9 ± 13.2
$V_{1/2(act)}$ (mV)	-47.8 ± 0.5	-48.7 ± 0.2	-50.1 ± 0.2
k	6.4 ± 0.5	6.3 ± 0.2	6.7 ± 0.2

G_{max} , maximum conductance; $V_{1/2(act)}$, voltage at which 50% of channels are activated; k, slope factor. There were no significant effects of ISO or ANP on I_{Na} G_{max} ($P=0.935$), $V_{1/2(act)}$ ($P=0.193$) or k ($P=0.955$). Data analyzed by one-way repeated measures ANOVA; $n=6$ myocytes.

References

1. Jaubert J, Jaubert F, Martin N, Washburn LL, Lee BK, Eicher EM, Guenet JL. Three new allelic mouse mutations that cause skeletal overgrowth involve the natriuretic peptide receptor c gene (npr3). *Proceedings of the National Academy of Sciences of the United States of America*. 1999;96:10278-10283.
2. Springer J, Azer J, Hua R, Robbins C, Adamczyk A, McBoyle S, Bissell MB, Rose RA. The natriuretic peptides bnp and cnp increase heart rate and electrical conduction by stimulating ionic currents in the sinoatrial node and atrial myocardium following activation of guanylyl cyclase-linked natriuretic peptide receptors. *Journal of molecular and cellular cardiology*. 2012;52:1122-1134.
3. Hua R, Adamczyk A, Robbins C, Ray G, Rose RA. Distinct patterns of constitutive phosphodiesterase activity in mouse sinoatrial node and atrial myocardium. *PloS one*. 2012;7:e47652.
4. Rae J, Cooper K, Gates P, Watsky M. Low access resistance perforated patch recordings using amphotericin b. *J Neurosci Methods*. 1991;37:15-26.
5. Mangoni ME, Couette B, Bourinet E, Platzer J, Reimer D, Striessnig J, Nargeot J. Functional role of l-type cav1.3 ca²⁺ channels in cardiac pacemaker activity. *Proceedings of the National Academy of Sciences of the United States of America*. 2003;100:5543-5548.
6. Zhang Z, He Y, Tuteja D, Xu D, Timofeyev V, Zhang Q, Glatter KA, Xu Y, Shin HS, Low R, Chiamvimonvat N. Functional roles of cav1.3(alpha1d) calcium channels in atria: Insights gained from gene-targeted null mutant mice. *Circulation*. 2005;112:1936-1944.
7. Azer J, Hua R, Krishnaswamy PS, Rose RA. Effects of natriuretic peptides on electrical conduction in the sinoatrial node and atrial myocardium of the heart. *J Physiol*. 2014;592:1025-1045.
8. Nygren A, Lomax AE, Giles WR. Heterogeneity of action potential durations in isolated mouse left and right atria recorded using voltage-sensitive dye mapping. *American journal of physiology. Heart and circulatory physiology*. 2004;287:H2634-2643.
9. Glukhov AV, Fedorov VV, Anderson ME, Mohler PJ, Efimov IR. Functional anatomy of the murine sinus node: High-resolution optical mapping of ankyrin-b heterozygous mice. *American journal of physiology. Heart and circulatory physiology*. 2010;299:H482-491.
10. Fedorov VV, Lozinsky IT, Sosunov EA, Anyukhovskiy EP, Rosen MR, Balke CW, Efimov IR. Application of blebbistatin as an excitation-contraction uncoupler for electrophysiologic study of rat and rabbit hearts. *Heart Rhythm*. 2007;4:619-626.
11. Farman GP, Tachampa K, Mateja R, Cazorla O, Lacampagne A, de Tombe PP. Blebbistatin: Use as inhibitor of muscle contraction. *Pflugers Arch*. 2008;455:995-1005.
12. Morley GE, Vaidya D, Samie FH, Lo C, Delmar M, Jalife J. Characterization of conduction in the ventricles of normal and heterozygous cx43 knockout mice using optical mapping. *Journal of cardiovascular electrophysiology*. 1999;10:1361-1375.
13. Egom EE, Vella K, Hua R, Jansen HJ, Moghtadaei M, Polina I, Bogachev O, Hurnik R, Mackasey M, Rafferty S, Ray G, Rose RA. Impaired sinoatrial node function and increased susceptibility to atrial fibrillation in mice lacking natriuretic peptide receptor c. *J Physiol*. 2015;593:1127-1146.

14. Marionneau C, Couette B, Liu J, Li H, Mangoni ME, Nargeot J, Lei M, Escande D, Demolombe S. Specific pattern of ionic channel gene expression associated with pacemaker activity in the mouse heart. *J Physiol.* 2005;562:223-234.

Effects of Wild-Type and Mutant Forms of Atrial Natriuretic Peptide on Atrial Electrophysiology and Arrhythmogenesis

Rui Hua, Sarah L. MacLeod, Iuliia Polina, Motahareh Moghtadaei, Hailey J. Jansen, Oleg Bogachev, Stacy B. O'Blenes, John L. Sapp, Jean-Francois Legare and Robert A. Rose

Circ Arrhythm Electrophysiol. 2015;8:1240-1254; originally published online July 30, 2015;
doi: 10.1161/CIRCEP.115.002896

Circulation: Arrhythmia and Electrophysiology is published by the American Heart Association, 7272 Greenville Avenue, Dallas, TX 75231

Copyright © 2015 American Heart Association, Inc. All rights reserved.
Print ISSN: 1941-3149. Online ISSN: 1941-3084

The online version of this article, along with updated information and services, is located on the World Wide Web at:

<http://circep.ahajournals.org/content/8/5/1240>

Data Supplement (unedited) at:

<http://circep.ahajournals.org/content/suppl/2015/07/30/CIRCEP.115.002896.DC1.html>

Permissions: Requests for permissions to reproduce figures, tables, or portions of articles originally published in *Circulation: Arrhythmia and Electrophysiology* can be obtained via RightsLink, a service of the Copyright Clearance Center, not the Editorial Office. Once the online version of the published article for which permission is being requested is located, click Request Permissions in the middle column of the Web page under Services. Further information about this process is available in the [Permissions and Rights Question and Answer](#) document.

Reprints: Information about reprints can be found online at:
<http://www.lww.com/reprints>

Subscriptions: Information about subscribing to *Circulation: Arrhythmia and Electrophysiology* is online at:
<http://circep.ahajournals.org/subscriptions/>